CHALMERS
UNIVERSITY OF TECHNOLOGY

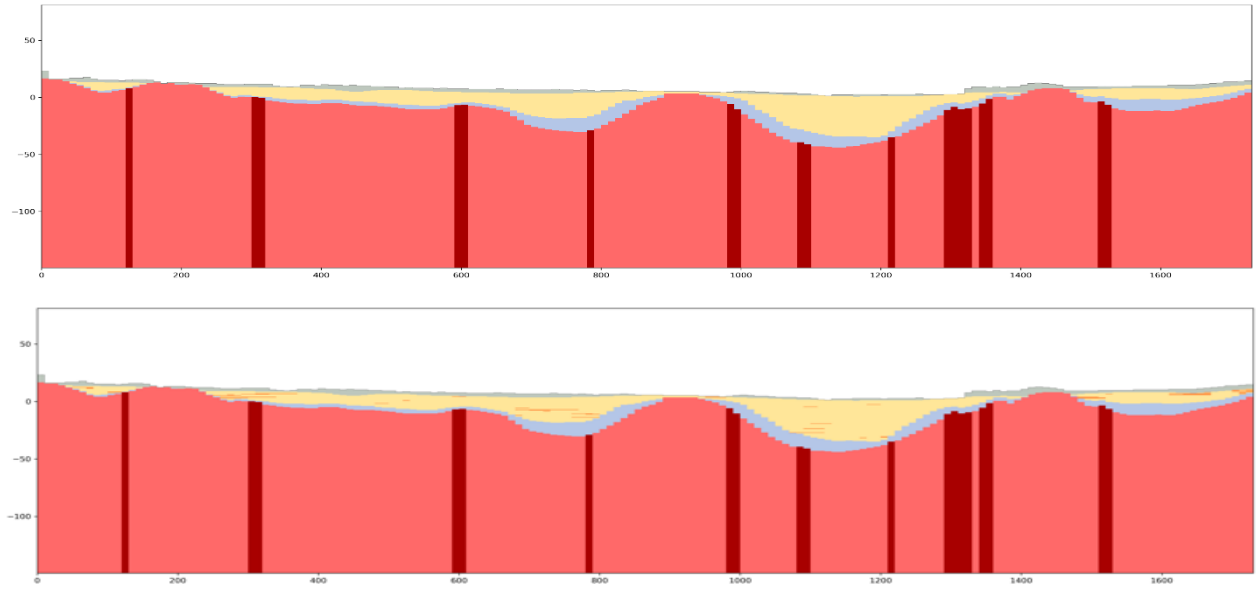

Evaluating the effects on pore pressure decrease from leakage in deep excavations when accounting for geological model uncertainty

Master's thesis in Infrastructure and Environmental Engineering

SOFIE AXEEN

Department of Architecture and Civil Engineering
Division of Geology and Geotechnics
Engineering Geology
CHALMERS UNIVERSITY OF TECHNOLOGY
Gothenburg, Sweden 2023
www.chalmers.se

MASTER'S THESIS 2023

Evaluating the effects on pore pressure decrease from leakage in deep excavations when accounting for geological model uncertainty

Master's thesis in Infrastructure and Environmental Engineering

SOFIE AXEEN

Department of Architecture and Civil Engineering
Division of Geology and Geotechnics
Engineering Geology
CHALMERS UNIVERSITY OF TECHNOLOGY
Gothenburg, Sweden 2023

Evaluating the effects on pore pressure decrease from leakage in deep excavations when accounting for geological model uncertainty

SOFIE AXEEN

Master's thesis 2023
Department of Architecture and Civil Engineering
Division of Geology and Geotechnics
Engineering Geology
Chalmers University of Technology
SE-412 96 Gothenburg, Sweden
Telephone: + 46 (0)31-772 1000

Cover:
Illustration of the two geological models included in this study. Retrieved from the modelling program MODFLOW illustrated with the add on code FLoPy.

Chalmers Reproservice
Gothenburg, Sweden 2023

Evaluating the effects on pore pressure decrease from leakage in deep excavations when accounting for geological model uncertainty

Master's thesis in Infrastructure and Environmental Engineering

SOFIE AXEEN
Department of Architecture and Civil Engineering
Division of Geology and Geotechnics
Chalmers University of Technology

ABSTRACT

Increased population and urbanization have led to challenges for many cities, as available land becomes increasingly limited. This has resulted in an increased interest in building underground facilities. During the construction of these facilities, there is a risk of groundwater leakage which can result in lowering of groundwater levels with subsequent ground subsidence and damage to buildings, infrastructure and other installations. It is therefore important to have a solid understanding and knowledge of the stratigraphy, the hydrogeological properties and thus potential flow paths for water within the building area. In Sweden, it is common to have thin sand layers embedded in clay layers that were formed during the end of the last ice age due to varying sea levels. These local and thin sand layers tend to be overlooked in groundwater modelling when attempting to predict pore pressure changes and settlement calculations. The aim of this work has therefore been to investigate how the inclusion of these sand layers affects forecasts of pore pressure changes as a result of leakage due to deep excavation. This has been done through numerical modelling based on two different geological conceptualisations, where the first model assumes that the clay is homogeneous and the second includes these sand layers. The flow models have been developed in MODFLOW and applied to a hypothetical shaft located at Korsvägen, Gothenburg.

The results show significant differences between the models, where the inclusion of sand layers results in faster pore pressure decrease in the clay while the pressure level in the lower aquifer increases. In addition, local differences were observed where the influence of the sand layers can both result in increasing and decreasing pore pressure, depending on their position and possible connectivity to the upper or lower aquifer. In summary, the results underline the importance of including these types of geological uncertainties, as they have an impact on pore pressure changes. Failure to consider these factors can potentially lead to underestimation of settlement risks and thus damage to buildings and other installations.

Keywords: groundwater modelling, uncertainties, MODFLOW, groundwater drawdown, pore pressure decrease,

Acknowledgements

This master´s thesis was performed as the final part of the Master Program Infrastructure and Environmental Engineering at the department of Architecture and Civil Engineering, Chalmers University. I would like to thank Christian Butron at Trafikverket and Johan Thörn at Bergab for providing material and data for the project. I would also like to thank Ezra Haaf and my examiner, Lars Rosén, for providing valuable input and feedback on the project. Finally, I would like to give a special thanks to my supervisor Johanna Merisalu for all her guidance and support during this project.

Sofie Axeen, Göteborg, Mars 2024

Contents

1. Introduction

This section presents an outline of the background, aim and limitations of the paper. It provides context, states the objectives, and acknowledges the scope of the research.

1.1 Background

Increasing population and urbanization cause land-use conflicts in cities worldwide where stakeholders compete over limited available surface area (Huggenberger & Epting, 2011). This means that underground facilities such as subways and garages are increasingly constructed to make space on the ground surface available for other more attractive purposes. During the construction of underground facilities there is risk of groundwater drawdown through seepage. Groundwater drawdown in confined aquifers can cause pore pressure decrease in overlaying soft soils which subsequently can lead to settlements and thereby damage subsidence sensitive buildings and facilities (Boone, 1996; Persson, 2007). Therefore, a thorough risk assessment including risk identification, risk analysis and risk evaluation is essential to properly managing the risk of groundwater drawdown (Tartakovsky, 2013; Sundell, 2018).

Groundwater drawdown entails that the stresses in the subsurface change. Simplified, the total stresses (σ_0) in the ground can be divided in-to stresses carried by the grain skeleton, effective stress (σ'_0), and residual stresses transferred in the liquid phase, pore pressure (u) (Sällfors, 2013). Groundwater drawdown leads to a reduction in pore pressure and an increase in effective stresses which can cause a volume change in the soil. The volume change that occurs when the pore pressure is reduced is called consolidation and can lead to ground settlement. In permeable materials such as sand, the pore pressure changes occur largely instantaneously. However, for materials with low conductivity such as clay, consolidation takes long time which means that the deformations are strongly time-dependent.

To be able to predict the risk of pore pressure changes, the effects of the underground construction on the groundwater levels in the confined aquifer and the pore pressure in the soft soil must be evaluated. Numerical groundwater modelling is a helpful tool for predicting and understanding how underground construction may affect groundwater levels (Sundell, 2016). One commonly used approach in numerical groundwater flow modelling is the layer-based approach where the stratigraphy is divided into layers representing different soil types (Moya et al., 2014). Conversely, this approach is not always suitable as thin and local hetrogenities risk being neglected or overestimated (Enemark et al, 2022). Traditionally, these models are based solely on one geological conceptualisation of reality, which means that uncertainties about for example geological conditions are ignored (Refsgaard et al., 2012). However, to enable valid results from a groundwater model, a solid understanding of the stratigraphy, the hydrogeological properties and thus the potential pathways of the groundwater within the area of interest are required.

Detailed investigations of the area are needed so that a reasonable estimate of the sequence and properties of the stratigraphic unit can be determined, and a representative conceptualisation of the area can be created. As geological investigations, e.g. test drilling, are often limited, knowledge of the geological history of the area is also required (Jørgensen et al., 2010). Western Sweden has a varied topography where a typical soil layer profile in a valley consists of patches of abrasion sand (beach deposits) and filling materials (in urban areas), postglacial and glaciomarine clay with an upper portion (up to a few meters) of dry crust, followed by a lower layer of lodgement glacial till, in some parts also glacio-fluvial deposits, and finally bedrock. An upper unconfined aquifer is typically developed in the sand and filling layers and a lower confined aquifer is developed in the glaciofluvial/glacial till deposits. The clay is usually normal to slightly over consolidated (Bjerrum, 1967; Larsson & Sällfors, 1995). The

sediments in the valleys are mainly of Quaternary origin and were formed during the deglaciation of the late Weichselian ice sheet (Lundqvist, 1983). From the deglaciation of the area, starting approximately 15,000 years before present, transgressions and regressions caused by land uplift resulted in variable shoreline positions over time (SGU, 2021). This meant that erosion and redeposition of glacial deposits resulted in thin layers of sand to be formed within the glaciomarine clay sequence.

The occurrence of permeable sand deposits within the clay may have a major impact on the hydrogeological response in the aquifer induced by leakage. These sand deposits are also often overlooked when predicting leakage and the subsequent groundwater drawdown and pore pressure reduction in these kinds of settings. Therefore, this report will investigate how the inclusion of local permeable soil layers can affect leakage, the rate of pore pressure reduction in the clay as an effect of excavation, and how the water level in the upper and lower aquifers can be affected. In this report, the term "aquifer" refers to permeable layers with potential high water flows but not necessarily suitable for water extraction. To evaluate the effects of sand layers within the clay sequence, two different geological conceptualisations have been used as input to two numerical groundwater models. The first model considers the clay sequence to be homogenous without sand layers while the second includes thin and local sand layers within the clay.

1.2 Aim

The aim of this study is to assess the effects on pore pressure decrease from groundwater leakage in deep excavations when accounting for geological model uncertainty by setting up two hydraulic models based on different geological conceptualisation of the stratigraphy. The difference being inclusion and exclusion of local permeable sand lenses, which is common in glaciomarine clay deposited during varying shoreline displacement. The following research questions are aimed to be answered:

- How can sand lenses within clay layers be included and well represented in the numerical groundwater model?
- Does the inclusion of sand lenses in the geological model affect the rate and magnitude of the pressure level changes in the upper and lower aquifer due to leakage?
- How does the pore pressure reduction rate and magnitude in the clay differ between the two models?

1.3 Limitations

The main limitations of this thesis are as follows:

- The development of geological models is outside the scope of this paper. Thus, already developed geological models were used for the groundwater flow models.

- No interpretation regarding the impact of variations in pore pressure on settlement rate and magnitude has been conducted.

2. Teory and methods

This section presents the methods used for groundwater modelling and relevant theory about groundwater modelling. The sections follow the structure of a general groundwater flow modelling process.

2.1 Groundwater modelling

A model is constructed by idealizing and simplifying a real scenario in order to represent reality as well as possible (Persson, 2007). A model can for example be a physical model such as a smaller representation of a building to visualize the design, or a mathematical model that calculates stresses in the load-bearing beams of the same building. Regardless of model sort, common to all models is that they are based on assumptions and simplifications, which result in uncertainties and thus cannot be seen as a truth.

In geotechnical and hydrogeological modelling, numerical models are frequently used. A step-by-step method for numerical groundwater modelling is shown in Figure 1. The first step is to identify the main objective of the model, which is often performed via one or more questions the model is aiming to answer. To identify the scope of the model is extremely important as it determines which equations should be governing and which type of modelling is suitable. Subsequent steps are presented in the sections below. Important to note is that the process is an iterative process meaning that there is no straight forward approach and steps might be redefined during the process.

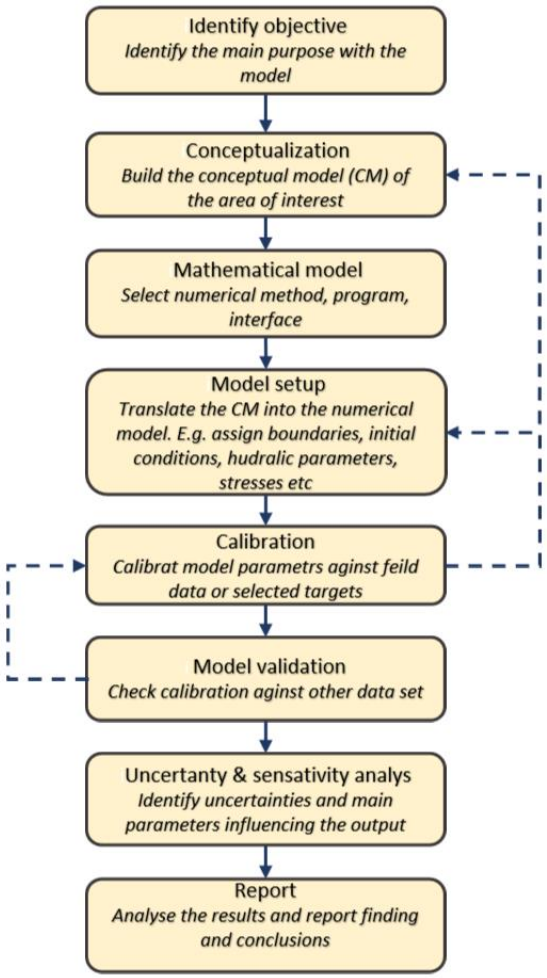

Figure 1. Flow chart of the process of groundwater modelling, with inspiration from Baalousha (2009).

2.2 Conceptualisation

When the objective of the model has been identified the second step in the groundwater modelling process is to conceptualize the area and system of interest. A conceptual model (CM) is a condensed description of the physical, hydrological, and geological processes that govern a groundwater system's behaviour, and it is the basis for creating a numerical groundwater model of the actual system (Anderson et al., 2015). Typically, field data, geology mapping, hydrologic analysis and expert judgment are used to create conceptual models. It is used to identify and categorize the primary characteristics and functions of the groundwater system, including areas for recharge and discharge, aquifer characteristics, hydraulic connections, boundary conditions, initial conditions, and interactions between surface water and groundwater.

2.2.1 Geological model

The backbone of the hydrogeological conceptual model is the geological model and the strategy for representing geological heterogeneity within the structural elements (Refsgaard et al., 2012). Traditionally, geological models are based on drillings, geophysical investigation and expert judgement. However, field investigations of the site conditions are both time consuming and expensive and the geological model must inevitably be built based on limited amounts of data which subsequently result in uncertainties (Zetterlund et al., 2011). Several geostatistical methods have been developed to estimate and simulate the soil strata at unsampled locations. There exist both estimation algorithms simulating the most likely soil condition and simulation algorithms that can generate an infinite number of equally probable realizations and thus account for the natural variability in the underground space (Bastante et al., 2008). There are two main geostatistical simulation approaches: the boundary-based approach and the category-based approach. The boundary approach uses continuous data to predict the position of the boundary between the stratigraphic units and assumes continuous stratigraphic units. If the stratigraphic units cannot be assumed to be continuous, a category-based approach is preferable. The category approach uses qualitative data such as geological descriptions to determine the material categories (Goovaerts, 1999). Since this approach is not limited by the material boundaries, it can generate a more complex stratigraphy including embedded materials (Xiao et al., 2017).

2.2.2 Boundary Conditions

To solve the groundwater flow equations boundary conditions need to be applied. Identification of boundary conditions in the conceptual model is one of the most important steps since this strongly governs flow direction and therefore the result (Anderson et al., 2015). Boundaries are often divided into three main types and according to Baalousha (2009) they can be defined as:

1) Specified head, also called Dirichlet or type I, and entails that the head in a cell is held constant:

$$h\,(x,y,z,t) = constant$$

2) Specified flow, also called Neumann or type II, and entails that the flow in a cell is held constant:

$$\nabla\, h\,(x,y,z,t,) = constant$$

When the flow is zero the boundary is often called no flow boundary and is often simulated by inactive cells in groundwater modelling.

3) Head-dependent flow, also called Cauchy or type III, and can described mathematical as follows:

$$\nabla\, h\,(x,y,z,t) + a*h = constant$$

where, *a* is a constant.

2.3 Numerical model

The next step in the groundwater modelling process is to select a suitable way to conduct compute groundwater flow. The main purpose of the model and the conceptual model is to provide a relevant basis for choosing and setting up a relevant mathematical model to solve the problem at hand. Since groundwater systems often are complex, numerical methods such as the finite difference method (FDM) are widely used (Baalousha, 2009). The governing equation used in FDM is as follows:

$$\frac{\partial}{\partial x}\left(Kx\frac{\partial h}{\partial x}\right) + \frac{\partial}{\partial y}\left(Ky\frac{\partial h}{\partial y}\right) + \frac{\partial}{\partial z}\left(Kz\frac{\partial h}{\partial z}\right) = Ss\frac{\partial h}{\partial t} - W \quad (1)$$

where,

W - the volumetric flow rate from sources and sinks
K - hydraulic conductivity in x,y, and z direction
Ss - Specific storage
h – the gradient of head
t - time

Equation 1 is based on Darcy's law and the conservation of mass principle and the assumptions that the groundwater has constant density, that the flow is saturated, and that Darcy's law applies, e.g. that the flow is laminar. There are several available numerical solvers that approximate groundwater flow that use FDM to solve hydrogeological problems and one commonly used tool is MODFLOW (Baalousha, 2009), which will be presented in the following section.

2.4 Model Setup

The next step in the groundwater modelling is to design the model. This step involves both translation of the conceptual model into the numerical model and to collect and select appropriate input data. Data collection is an essential step in the modelling process since the accuracy and representativeness of the input data affects the reliability of the model results (Anderson et al., 2015). Often various methods for data collection are used, such as field measurements, laboratory analysis and existing data sources. Field measurements involve direct measurements of hydrogeological properties on site such as hydraulic conductivity, porosity and water levels. Techniques for this can be pumping tests, slug test and test drilling such as cone penetration test (CPTs). Samples from the site can also be collected and analysed in a laboratory, to estimate parameters such as specific yield and hydraulic conductivity. However, these kinds of test are often limited since they are expensive and time consuming (Refsgaard et al., 2006) and therefore it is important to use and interpret available data from open data sources.

When the data needed is collected the discretization of the model and how to assign selected parameter must be evaluated. The two most commonly used approaches in groundwater modelling to assigning hydrogeological parameters in the model discretization are the layer approach (Moya et al., 2014; Polomčić et al., 2013) and the voxel approach (Jørgensen et al., 2015; Stafleu et al., 2011). Layer models divide the stratigraphy into layers representing different soil types whereas voxel models divide the soil into a structured mesh of volumetrics pixels (voxels) where each cell can be assigned a soil type, see figure 2.

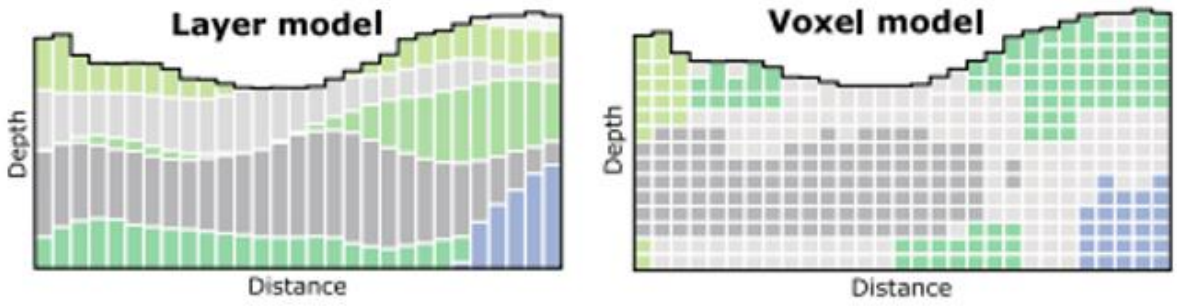

Figure 2. Illustrating a layer-based approach to the left and to the right a voxel approach. Modified figure from Enemark et al. (2022).

The layer-based model is not always suitable for complex geological settings, see Jørgensen, (2015) and Turner, (2006), as thin layers often are neglected or overestimated. Enemark et al., (2022) found, when comparing the layer and voxel approach, that the voxel approach in higher degree led to isolation of Quaternary sand lenses within the clay. Voxel models also often use more cells meaning that the time to run the simulation could be considerably longer and more complex.

2.4.1 MODFLOW

One of the most widely used groundwater modelling programs based on FDM is MODFLOW (Baalousha, 2009) developed by the U.S. Geological Survey (USGS) and released in the 1980s (McDonald & Harbaugh, 1983). It has since then undergone numerous updates and improvements and is available in different versions with different applications (Niswonger et al., 2011). The source code is free to download and can be used in several external interfaces such as Visual MODFLOW or Groundwater Model Systems (GMS). An alternative approach to using an external GUI (Graphical User Interface) is to use the programming language Python to create a MODFLOW model (Bakker et al., 2016). In Python there is a series of pre-coded subroutines group in what is called packages. These packages are built to represent various features in the groundwater system (Harbaugh, 2005). The RIV package for example is constructed to simulate the interaction between the groundwater and the surface water in a river. There are also several different packages that write input files that can be used to run the model in MODFLOW. Through combination of these pre-coded packages and external code the conceptual model can be built into a model that represents the area of interest.

2.5 Calibration and verification

Calibration is one of the last steps in groundwater modelling process and is conducted to adjust parameters and variables to accurately represent the behaviour of the real-world groundwater system being modelled. In groundwater modelling field measurements of head is often used to adjust the resulting heads from the model so that they match the field values (Baalousha, 2009). The *Root Mean Square Error* (RMSE) is a common statistical measure used in calibration of groundwater models and is calculated as in equation 2 below.

$$RMSE = \sqrt{[\frac{1}{n}\sum_{i=1}^{n}(h_{obs,i-}\, h_{sim,i})^2\,]} \quad (2)$$

Calibration is used to minimize the RMSE in equation 2, where h_{obs} is the observed or target value and the h_{sim} is the simulated value from the model (at location i). This means that a parameter such as hydraulic conductivity and recharge are changed to achieve as low RMSE as possible or an acceptable

error level. Calibration is mainly done automatically but can also be done manually. Automatic calibration can be conducted by software such as PEST (Doherty, 2015) and UCODE (Hill & Tiedeman, 2006), where every calibration can result in several calibrated model solutions that represents plausible conditions (Sundell et al., 2019). Regardless of how the calibration is performed the calibrated model should satisfy a proper match between simulated and observed head, representative water balance, alike gradient as observed in field and a similar behaviour for any data set (Baalousha, 2009).

Next step in the modelling process is to check if the model behaves similarly for any data set. Since the calibration process includes changing different parameters, such as hydraulic conductivity, it is important to validate that the model works as expected. A common way to do this is to use one part of a data set to calibrate the model, while the other part is utilized to evaluate the calibrated model, e.g., by evaluating other positions for head measurements and see if the simulated heads in these positions correspond to field measurement. Alternatively, calibration against one time period can be conducted and validated against another, such as comparing average yearly heads with short-term measurements. However, Doherty and Hunt (2010) note that while these exercises show that a calibrated model may mimic some system response under field conditions, the data utilized in a verification exercise often are more beneficial when incorporated into the calibration process.

2.6 Uncertainty and sensitivity

The next steps in the groundwater modelling process are to analyse the uncertainties and sensitivity of the model. Since models are interpretations of real-world systems uncertainties are inevitable. However, with knowledge and transparency about uncertainties and sensitivity, results from the model can give insight about risk and possible outcomes and stakeholders can decide if more resources should be spent on improving the quality of information or if risk-reducing measures should be implemented (Refsgaard et al., 2005).

The nature of uncertainties can be divided into two main categories: 1) the aleatory uncertainty and 2) the epistemic uncertainty (Ross et al., 2009). Aleatory uncertainty refers to inherent variability or the randomness that exists within a system or process. This type of uncertainty cannot be eliminated or reduced through additional information or analysis. Examples of aleatory uncertainty can be natural variation in groundwater recharge due to climate variability, or spatial heterogeneity of subsurface geological formations.

In contrast to aleatory uncertainties, epistemic uncertainties can be reduced by increased knowledge. As an example, knowledge about geological heterogeneity can be increased by conducting additional borings and other field investigations. Another example is that the epistemic uncertainty of the mean value of hydraulic conductivity can be reduced by gathering more information through site-specific research or in-situ investigations. However, gathering information is often time consuming and expensive and is therefore often limited (Zetterlund et al., 2011), resulting in substantial epistemic uncertainties. Uncertainties can be represented by statistical distributions and managed with probabilistic techniques, such as Monte Carlo simulations. This applies to both aleatory and epistemic uncertainty.

Another way of categorizing uncertainties in groundwater modelling is by their location (Refsgaard et al., 2006; Walker et al., 2003). These locations or sources can be categorized into five different categories: 1) Context and framing uncertainty, 2) Input uncertainty, 3) Model structure uncertainty, 4) Parameter uncertainty, and 5) Model technical uncertainty.

Context and framing uncertainty refers to uncertainties that arise from how a problem or decision is defined and framed. These uncertainties arise early in the process and should be addressed with consideration of the broader context and framing of the problem.

Input uncertainties are linked to driving forces and system data used in the model. These can be created due to insufficient information or poor quality, and it is therefore important to investigate what type of data is needed.

Model structure uncertainty refers to uncertainties due to the conceptualisation of the modelled system. These arise due to an insufficient comprehension, inadequate information, and oversimplifications of the modelled system in contrast to reality.

Parameter uncertainty is the uncertainty related to parameter values. These values are numerical values representing the characterization or properties of the system under consideration.

Model technical uncertainty is the uncertainty that results from the model being implemented by a computer, such as due to numerical approximations, resolution in space and time, and software flaws.

Input parameters can have a varying effect on the result of a simulation. It is therefore important to get an understanding of which parameter values that largely impact the results. This understanding can subsequently form the basis for decisions on e.g., if and what data to collect to reduce uncertainties in the model (Anderson et al., 2015). Which parameters that have a large impact on the model output can be identified and investigated with a sensitivity analysis. This type of analysis can be performed both locally or globally, meaning either on selected parameters of interest or on all parameters used in the model.

3 Case study and method applications

In this section, the study area and method applications will be presented. The section will start with a general description of the study area pursued by the model description following the steps of the groundwater modelling process.

3.1 Study area

The study area is located in central Gothenburg on the west coast of Sweden, see figure 3. The area is 1.58 km from north to south and 1.73 km from west to east. The topography is varying, with higher elevations at the east and southwest forming two main valleys that transfer into a relatively flat landscape in the northern part of the area. In the larger valley the River *Mölndalsån* is flowing. The land use in the area constitutes an urban city with buildings and infrastructure such as roads, rails, and pipes, which leads to a high proportion of impervious land. The area is a part of the ongoing underground project *Västlänken* in Gothenburg, hence there are many investigations and information of the geological and hydrogeological conditions available about the area.

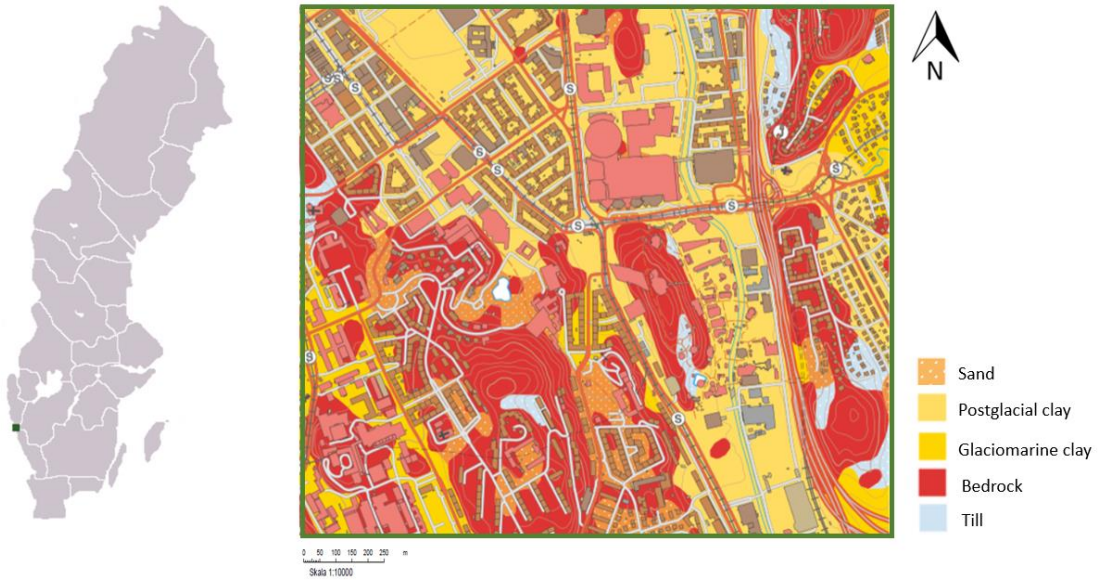

Figure 3. Location and illustration of the study area. The map shows the soil types, buildings, roads, railways, subway stations and elevation SORCE: GSU (Geological Survey of Sweden).

The hydrogeology in the area is characterized by exposed bedrock in the elevated areas and clay-filled valleys. Generally, the soil layers at the ground surface are made up of filling material, which rests on patches of abrasion sand (beach deposit) and a relatively thick layer of postglacial and glaciomarine clay with a dry crust in the upper part of the clay. Under the clay there is normally a layer of glacial lodgement till on top of the bedrock. Within the clay layer, thin and local sand layers formed during the regression and transgression of the latest ice age are present. The till constitutes a lower confined, partly leaking, aquifer and the filling, sand and the dry crust in clay constitutes an upper unconfined aquifer. The sand deposits within the clay sequence can constitute intermediate confined aquifers. The lower and upper aquifer are connected in the areas adjacent to bedrock outcrops.

3.2 Conceptualisation

The size of the area (1.58x1.73 km^2) has been chosen so that the edges will not be affected by the expected drawdown caused by the excavation. The water balance is represented by the inflow, outflow, and storage of water. The inflow is mostly governed by the inflow of water in the south and the recharge

from precipitation. The recharge to the lower aquifer from precipitation is expected to mostly occur in areas with bedrock outcrops where the lower and upper aquifers are connected and have direct contact with the atmosphere. The outflow is mainly at the northern border and the excavation, although surface water is also flowing out of the model by the river *Möndalsån* in the eastern valley. The excavation has been located in line with a planned underground train station in Gothenburg. The open shaft is 140x60 meters and extends to a depth of 20 meters from the ground surface, although the excavation walls are continuing 2 meters down into the bedrock. It should be noted that the extent of the excavation does not correspond to the actual excavation for the planned train station.

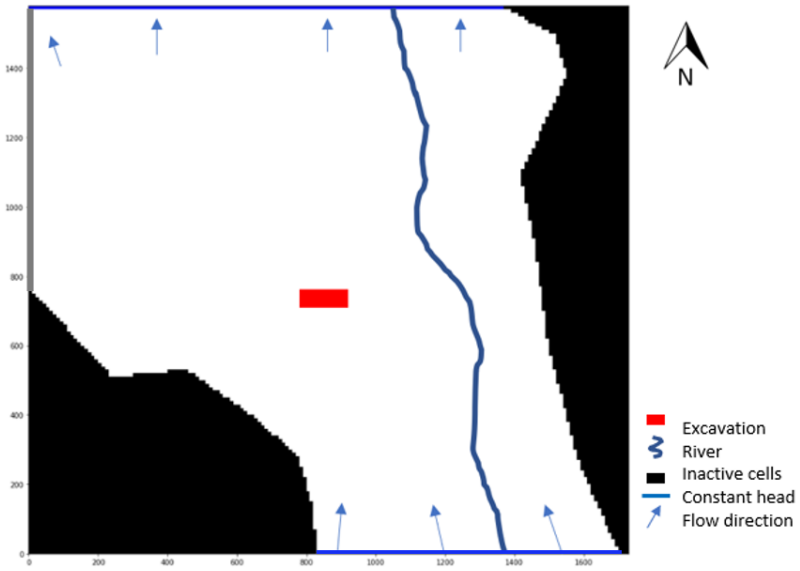

Figure 4. Illustration of the hydrogeological conceptualisation of the study area.

In figure 5 a conceptualisation of some of the feasible effects that the sand lenses may have on the water flows is illustrated. In Case I, the sand lenses have no connection to the upper or lower aquifer and can therefore be seen as an intermediate confined aquifer. These types of sand layers are expected to have a low impact on the pore pressure changes due to the leakage into the excavation if there is no direct contact with the excavation walls. However, if the excavation is located in contact with these types of sand layers, the pore pressure reduction in the clay is expected to go faster as the sand layers are working as a drain for the surrounding clay.

In Case II the sand layers are linked to the lower aquifer and can therefore be considered an extension of the lower aquifer. When there is a decrease in pore pressure within the lower aquifer, it is highly probable that a corresponding drop in pore pressure will occur within the interconnected sand lenses. These sand lenses effectively extend the influence of the lower aquifer higher into the adjacent clay layers, resulting in a propagation of reduced pore pressure. Consequently, these types of sand lenses have the potential to increase the risk of settlement-related structural damage to buildings.

In Case III the sand lenses create a connection between the upper and lower aquifers, potentially acting as a recharge pathway for the lower aquifer. This aids in stabilizing the groundwater level in the lower aquifer and subsequently prevents drawdown caused by a decrease in pore pressure in the overlaying clay. However, for the sand layers to function as a pathway to the lower aquifer, the sand lenses need to be well connected and located in areas conductive to infiltration. Therefore, Case III scenarios are anticipated in regions with thinner clay layers and permeable land use patterns.

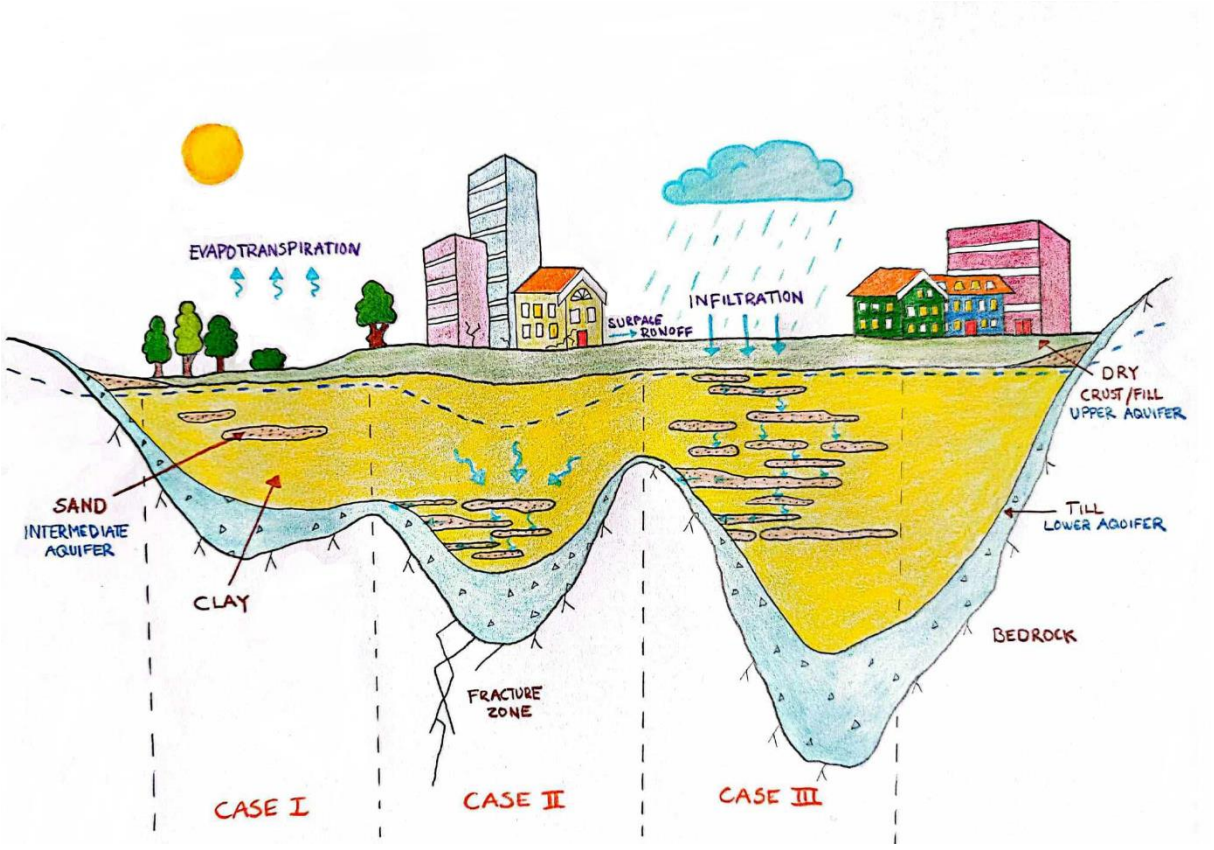

Figure 5. Illustrates a typical cross section for the stratigraphy and different scenarios that the sand layers might have. The dash line represents the pore pressure in the clay layer.

3.2.1 Boundary conditions

The lower boundary in the models, as well as the mountain ridges constituting water divides in east and west, is assumed to be a no flow boundary. In the north the boundary is represented by a constant head and has been applied with a general water level a few meters below the ground surface in order to imitate the outflow that occurs in this part of the area. In the south, the boundary is also represented by a constant head boundary. The constant head is assumed to be 2 meters below ground surface with a maximum of 30 m.a.s.l. in the more elevated areas. This represents the natural groundwater flow from the south to the north. The river *Möndalsån* has been represented with a head dependent flux boundary. The process of assigning boundary conditions to the models has been a highly iterative process where simulations have been run to evaluate if the applied boundary conditions are representing the area as accepted.

3.2.2 Geological model

The two geological models both consist of bedrock, fracture zones, till, clay, and fill. In figure 6 a cross section of the geological model for the two models can be seen. It can be seen that the only geological difference between the two models is the inclusion of local sand layers in model 2.

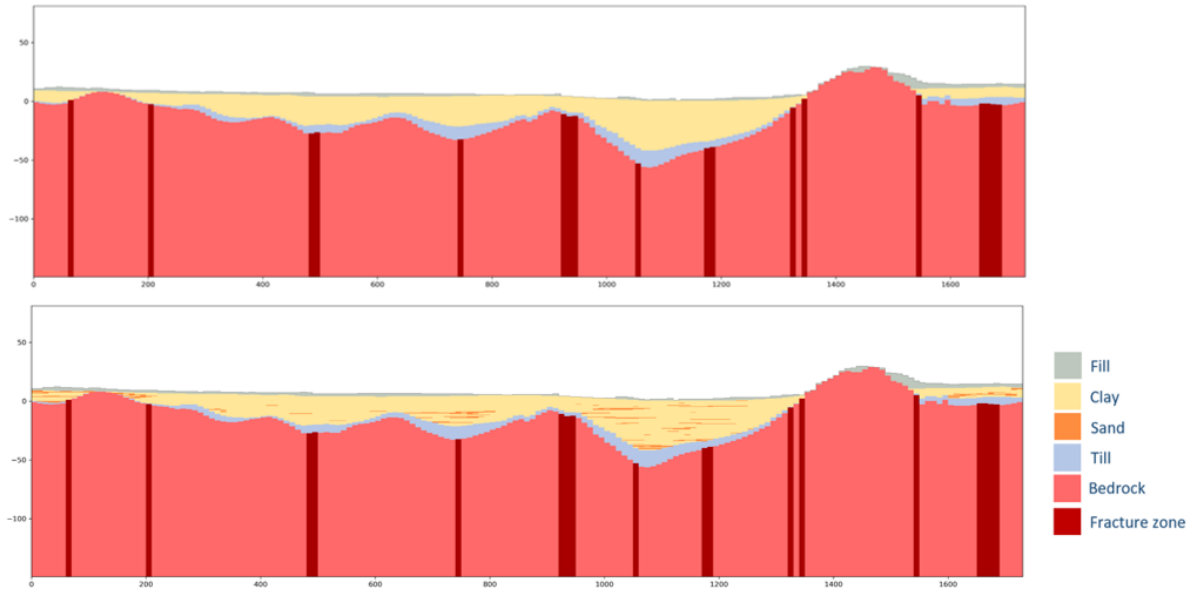

Figure 6. Illustrations of the geological conceptualisation. The cross section at the top shows the soil types for model 1- without sand and the cross section at the bottom shows the soil types for model 2 – with sand.

The fracture zones illustrated in the figure are based on data from SGU about the weakness zones in the bedrock surface. These fracture zones are generally in a non-vertical direction and are believed to likely exhibit some tilt. However, this fact has been neglected in the modelling process since it complicates the model. Instead, a vertical fracture zone is assumed to still provide a representative rendering of the water flow paths.

3.3 Numerical model

The numerical groundwater flow models have been created with the program MODFLOW. No graphical user interface has been used. Instead, the model is a scripted model with the programming language Python, and to run and postprocess the model FloPy has been used. MODFLOW comes in many different versions and MODFLOW-NWT has been used. One of the main differences between other MODFLOW versions and MODFLOW-NWT is that the Newton formulation allows cells where the head falls below the bottom elevation of the cell to stay active (Boyce et al., 2015). This is a very important feature since the excavation is designed to remove all water entering, which will reduce the head in the cells. If these cells become inactive (no-flow boundary), this would be counterproductive to what was tried to be achieved with the model. The pre-coded packages used in the models are: DIS, UPW, BAS, RIV, RCH, DRB, HFB, OC, and NWT. The applications and parameters used will be further presented in the following section.

3.4 Model setup

The model setup can be divided into two parts, where the first was to translate the received geological model into a groundwater flow model in MODFLOW using Python. The full script for this can be seen in Appendix C. The next part was to build the actual model to represent the area based on the conceptual model. Each pre-coded package used, and the input parameters will be presented in the following sections, and those not mentioned were kept as defaults. More extensive information about the packages and source code can be found at the Online MODFLOW Guide. The full script for this can be seen in Appendix D.

3.4.1 Translation

The geological model was received as a dat-file consisting of coordinates for x-,y- and z-direction as well as an indicator corresponding to each soil type included in the models. The geological model was built as a voxel model with a cell size of 10x10 in the x- and y-direction and 0.5 meters in the z-direction, resulting in about 8 million cells. The soil types and indicators were 1 - Sand, 2 - bedrock, 3 - till, 4 - clay, 5 - filling, 6 - above ground surface, and 7 - fracture zones in the bedrock. Since a layer-based model, which is common in groundwater modelling, could overestimate the thickness and extent of the sand lenses, the model is kept as a voxel model with the same cell size.

The only adjustment from the geological model was that the cells with indicator *above ground surface* were excluded, creating a model top with varying topography. To translate the geological model, the locations for each indicator have been translated into a corresponding layer, row, and column. The script then iterates over each cell, identifying and assigning the corresponding indicator and the results were saved as a NumPy array.

3.4.2 DIS

The discretization package (DIS) was used to assign the grid, time and length units, and time discretization. The size of the cells was as mentioned kept the same as in the geological model, resulting in 295 layers, 158 rows, and 173 columns. The time unit was selected to be days and the length was in meters.

To be able to evaluate if the inclusion of sand lenses leads to faster pore pressure changes, a transient simulation must be conducted. Since sand has relatively high hydraulic conductivity the changes occur largely instantaneously, hence the stress periods have been chosen to be 1 day, 1 week, 2 weeks, 1 month, 1 year, and 30 years. An additional stress period called 0 days was also included where the drains (see section DRN) in the model were inactive. This to be able to retrieve reasonable starting head values that were not impacted by the excavation and thus enable a better evaluation of the pore pressure changes caused by the leakage to the excavation.

3.4.3 UPW

The Upstream Weighting Package (UPW) was used to specify the properties controlling the groundwater flow between cells. The upstream-weighting method in the UPW package is different from other flow-controlling packages available in MODFLOW. Instead of using hydraulic heads from both neighbouring cells to calculate flow between them, the upstream weighing approach uses only the hydraulic head in the cell where water is flowing from. This helps prevent unrealistic scenarios where water flows out of dry cells. The parameters defined in the UPW package were hydraulic conductivity (*hk*), vertical conductivity (*vk*), specific storage (*Ss*), and specific yield (*Sy*).

Since the area is a part in the ongoing project *Västlänken* there were several available reports and investigations on hydrogeological parameters. The values assigned in the model are presented in table 1. These are the same or within the same interval presented and used for a groundwater model conducted by the Swedish National Transport Administration, *Trafikverket,* and presented in Trafikverket (2016).

Table 1. Vertical and horizontal conductivity, specific storage, and specific yield for the different soil types.

	hk (m/d)	vk (m/d)	Ss (1/m)	Sy (1/m)
Sand	3.0	3.0	1.50E-04	1.00E-01
Bedrock	0.0035	0.0035	4.00E-07	1.00E-03
Till	3.0	3.0	1.50E-04	1.00E-01
Clay	0.000086	0.000043	1.00E-07	1.00E-03
Fill	0.86	0.43	1.00E-04	7.00E-02
Fracture zones	0.43	0.43	4.00E-07	1.00E-03

3.4.4 BAS

The Basic Package (BAS) was used to assign starting heads and boundary conditions of type I and II. The initial heads for model 1 and model 2 were based on a steady state simulation without external stress from the excavation. This steady state simulation was made without the inclusion of sand lenses. The assumed starting heads for this simulation were based on the groundwater level in the upper aquifer and assume to be the same with depth. The groundwater level in the upper aquifer is according to Trafikverket (2016) identified to be about 1-1.5 meter below ground surface. However, due to the high urbanisation in the area there are expected to be a high amount of drainage in the subsurface. Therefore, the initial groundwater level has been chosen to 2 meters below ground surface.

When assigning a type I boundary condition (constant head), the gradient to the connecting cell is the governing if water will flow out or into the model. To ensure that the constant head boundary in the northern part of the model were simulating an outflow of water the constant head as been assigned to be at 0 m.a.s.l. which is a few meters below the ground surface.

To be able to assign a reasonable constant head at the southern border, the inflow at this boundary had to be estimated. To estimate the inflow (Q) at the southern border Darcy´s Law has been used.

$$Q = KAi \qquad (3)$$

where,

K – hydraulic conductivity
A - Area
i – gradient

The gradient has been estimated by looking at the elevation from the border and 2000 meters upstream. It is assumed that the gradient of the groundwater level is similar to the topography, with the exception of high elevations. The elevation can be seen in figure 7, and the estimated gradient is calculated at 1%.

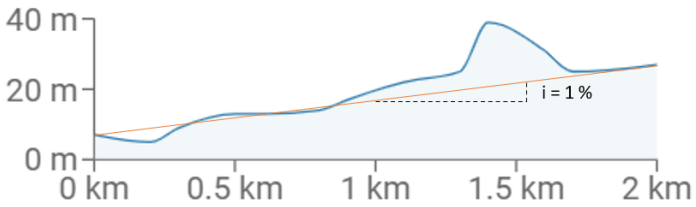

Figure 7. Illustration of the elevation upstream the study area. SORCE: Lantmäteriets map service.

The flow was calculated based on the area and conductivity for each soil type and the calculated flow is presented in table 2. The estimation of the total inflow should however not be seen as an exact value but rather as an estimate of the proportion of the inflow.

Table 2. Presents the highest and lowest hydraulic conductivity used in Trafikverkets model, the area and the calculated flows based on the different hydraulic conductivity for the different soil types.

	hk_{min} (m/day)	hk_{max} (m/day)	Number of cells	Area (m^2)	Q_{low} (m^3/day)	Q_{high} (m^3/day)
Sand	0,86	6,05	13	65	0,6	3,9
Bedrock	0,0035	0,017	22 778	113 890	3,9	19,7
Till	0,86	6,05	600	3 000	25,9	181,4
Clay	0,0043	-	983	4 915	0,2	0,2
Filling	0,086	6,05	269	1 345	1,2	81,3
Fracture zones	0,052	0,017	1 022	5 110	2,6	0,9
			Total inflow:		34	287

Based on the calculated Q_{low} and Q_{high} the inflow at the southern border was estimated to be within the range of 50-350 m^3/day. The constant head at the southern border was therefore chosen to be 4 meters below the ground surface with a maximum at 30 m.a.s.l., which resulted in an inflow within this interval for all time periods.

3.4.5 RIV

To simulate the river *Mölndalsån*, the head dependent flux boundary package River (RIV) has been used. The RIV package uses two elevations, one representing the bottom elevation of the river and the other representing the head of the river. If the head in a connecting cell is above the bottom of the river, water will either flow into or out of the river, depending on whether the head in the connecting cell is higher or lower than the one defined as the river head. Since *Mölndalsån* is in the eastern valley which contains a thick clay layer the RIV package has been used to reduce the groundwater table and prevent it from exceeding the ground surface. This has been done by assigning the head of the river to the elevation of each cell in the river to correspond to the model top.

3.4.6 RCH

According to Trafikverket (2016), an expected net recharge for the area is 50-350 mm/year. This is based on the yearly precipitation, evapotranspiration, surface runoff for the different land uses in the area, and some additional recharge due to leakage from drinking water distribution systems. The recharge

was assigned using the recharge package (RCH). The RCH simulates the specified flux at the top of the model (or first active cell) and the recharge is calculated based on the area of the cell.

Since there were areas with clay in the first layer the flow governing properties in these cells has been change to the same as for soil type- filling. This is to ensure that no extensive water is building up due to the low conductivity of clay. The assigned recharge in the area has as mentioned been based on the different land uses in the area, and therefore different recharge rates have been assigned to different soil types.

3.4.7 DRN and HFB

The drain package (DRN) and Horizontal Flow Barriers package (HFB) have been used to simulate the open shaft. The DRN package simulates head-dependent flux boundaries. It works similarly to the RIV package except if the head at a cell falls below the assigned threshold, no flux will enter the model. This means that the package only simulates outflows from the model. The parameters in the DRN have been assigned to simulate that all water that enters the excavation will be removed. The drains have not been included in the steady state simulation.

In order to simulate the walls of the excavation the HBF package have been used. The package allows the hydraulic conductivity to be reduced between cells. This is assigned with the parameter *hydch*r which is the hydraulic conductivity divided by the width of the horizontal flow barrier. This parameter has been assigned the value of 1,0E-13 in the models.

3.4.8 OC and NWT

The output control package (OC) was used to control which outputs would be saved from the simulation. The printed and saved outputs were drawdown, head, and budget. The solver used in the models was the Newton solver (NWT). This is the solver conducted for MODFLOW-NWT and it only works in combination with the UPW package. The XMD matrix solver was assigned since this is developed to handle simulations including drains. Since the models are complex and relatively large, the maximum number of iterations was increased to 250 and the maximum head change between iterations to 0.01, compared to the default values of 100 and 1e-4.

3.5 Calibration and verification

Since the main purpose of this study was to compare the results from two different conceptualisations of stratification, only manual calibration has been used. An automatic calibration with e.g. PEST can result in an almost infinite number of solutions where parameter values can vary. This means that automatically calibrated models, even if calibrated against the same values, could become different and the comparison between the two models could be misleading. However, the modelling process is a highly iterative process, and a manual calibration has been performed.

The manual calibration was not executed against real measurements from the area, with for example the RMSE approach. This because it was considered to be outside the scope of this paper. To compare the two models, it was not necessary to represent the area in such detail. Since the area is highly urbanised there are many stresses affecting the groundwater system that have not been considered in the models, such as existing tunnelling, leaking pipes and artificial recharge facilities. In order to calibrate against real measurements such stresses had to be taken into consideration, thereby increasing the complexity of the system in a way that was judged to be irrelevant to the aim of the study and too time consuming.

The manual calibration was conducted as an iterative process, to find a suitable combination of parameters. Parameter changes have been done one at a time to understand how the change affect the result. Starting heads, constant head boundary, inflow, recharge, hydraulic conductivity for all soil

types, hydraulic conductivity for the HFB, and conductance for the drains have been used as calibration parameters.

3.6 Uncertainties and sensitivity

Since the aim of the analysis was to investigate and evaluate changes in pore pressure due to two different conceptualisations and not to represent an actual existing groundwater system, no further uncertainty analysis has been made.

During the calibration of the model, it was also possible to identify the sensitivity of the parameters used. When the calibration was finalised, these identified parameters were changed again to evaluate if there were effects on the result and how large these changes were.

4 Results

In this section, the results from the simulations of the two different models will be presented. The results will be presented for 8 comparison points where the pore pressure change in the clay sequence is graphically depicted.

4.1 Location and stratigraphy

In Figure 8 the locations of the observation points are shown. On the north and south sides of the excavation four points with different distances from the excavation have been chosen. The points are located in the same valley as the excavation and have different stratigraphy, including variations in clay thickness, the presence of sand lenses, and potential connections to both upper and lower aquifers. This diversity enables evaluation of the effects of different types of sand lenses.

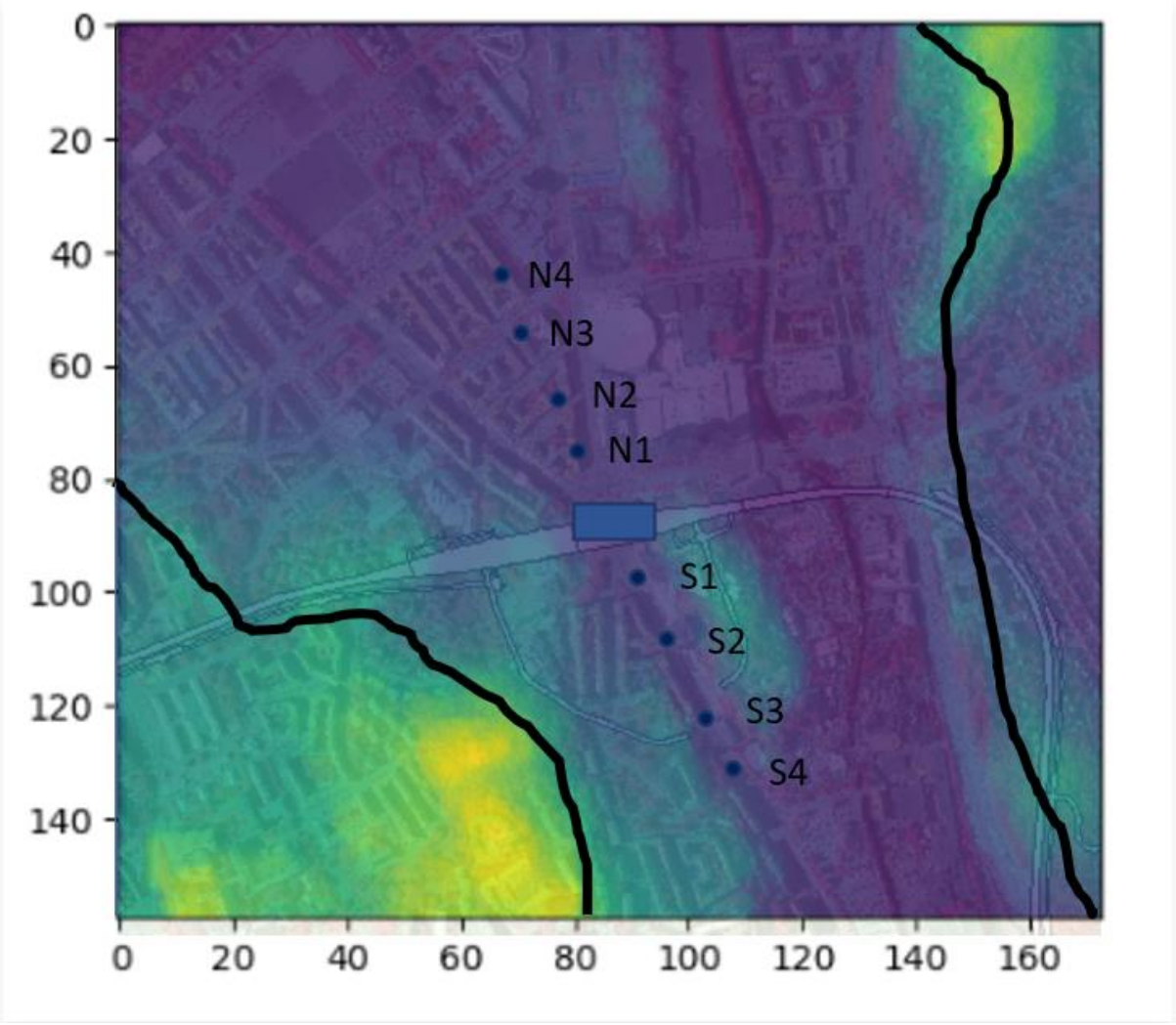

Figure 8. Illustration of the model area and the location for the observation points. The black lines represent the no flow boundaries, the blue points are the location for the observation points (N1-4 and S1-4) and the blue rectangle is the location of the open shaft.

In Figure 9 the stratigraphy of the northern observation points is illustrated. The figure is illustrating *model 2 – with sand,* however *model 1 – without sand* has the same layering but without the sand layers, and instead it is a homogeneous clay layer. The depth of the clay layer on the north side of the excavation is about 20-25 meters and the lower aquifer is about 10 meters thick but decreases in thickness closer to the excavation. More information on the surrounding area of the observation points

can be found in Appendix A, where a cross section of the model area for each observation point can be seen.

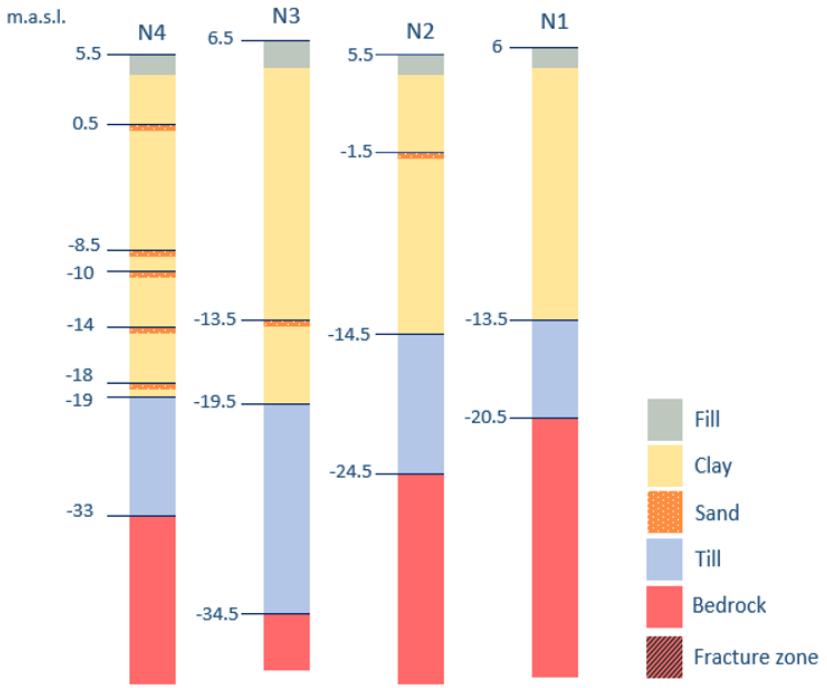

Figure 9. Illustration of the stratigraphy of the northern observation points.

Error! Reference source not found. illustrates the stratigraphy of the observation points south of the excavation. Here it can be seen that the thickness of the clay layer and lower aquifer is greatly reduced

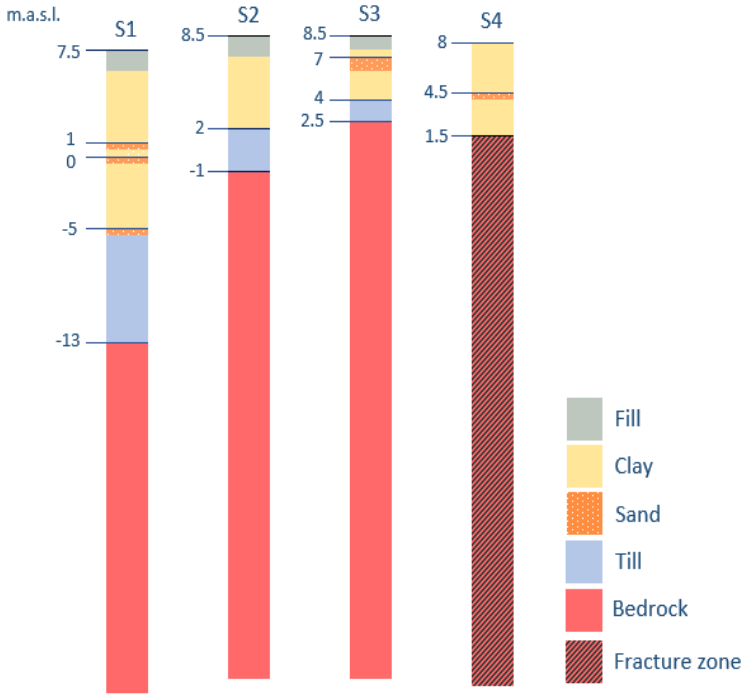

Figure 10. Illustration of the stratigraphy of the southern observation points.

compared to the northern side and at point S3 the depth from the ground surface to the bedrock is a total of 5 meters.

4.2 Pore pressure change

In the northern observation points clear differences between pore pressure reduction with and without sand lenses can be seen over time (Figure 12). The reduction in *model 1 – without sand*, follows a more general pattern where it is lowest at the top and increases linearly down to the lower aquifer where it remains constant with depth. For *model 2 – with sand,* the reduction is much more disjointed and the sand lenses result in both a higher and lower reduction in pore pressure compared to model 1.

In observation point N4 (Figure 11a), the sand layers exhibit varying impact throughout the depth of the clay. Within one day, the middle sand layer is responding with a similar reduction as the lower aquifer (as shown at the bottom of the graph) suggesting a connection between this sand lens and the lower aquifer, as in case II in figure 5 (section 3.2.2). Subsequently, after one week, the divergence in reduction between the models at this sand layer becomes more pronounced, and with the reduction spreading to the surrounding clay. Conversely, other sand layers, such as those situated at depths of -5 and -20 meters, appear to act as barriers to this propagation, resulting in a slower reduction rate. However, in the long term these effects fade, and after 1 year, the pore pressure reduction is significantly higher in the whole clay sequence in the model including sand compared to model 1 – without sand.

The sand lens at observation point N3 (Figure 11b) is also counteracting the reduction in pore pressure in the surrounding clay, and short term the reduction is smaller at the depth of the sand lens and the surrounding clay. This suggests that this layer acts as an intermediate aquifer without any connection to the lower or upper aquifer as in Case I in Figure 5. However, after two weeks the counteracting effect has faded, and the reduction is higher for the whole clay sequence for the model including sand. The same type of sand lens can also be seen at observation point N2 (figure 11c), but here the sand lens is located at a higher level leading to a slower reduction rate. First after 1 year, the reduction in pore pressure is higher for the model including sand, showing that the same type of sand lens can have different effects depending on its location.

At observation point N1 (Figure 11c) there is an absence of sand layer present in the stratigraphy. However, there are still small differences in pore pressure reduction between the models. The reduction of the pressure level in the upper aquifer is after one week higher for the *model 1 – with sand* and for the lower aquifer it is smaller. This variation suggests the potential for additional recharge from the upper to the lower aquifer, indicating the presence of sand layers resembling Case II, as illustrated in Figure 5, within the model area.

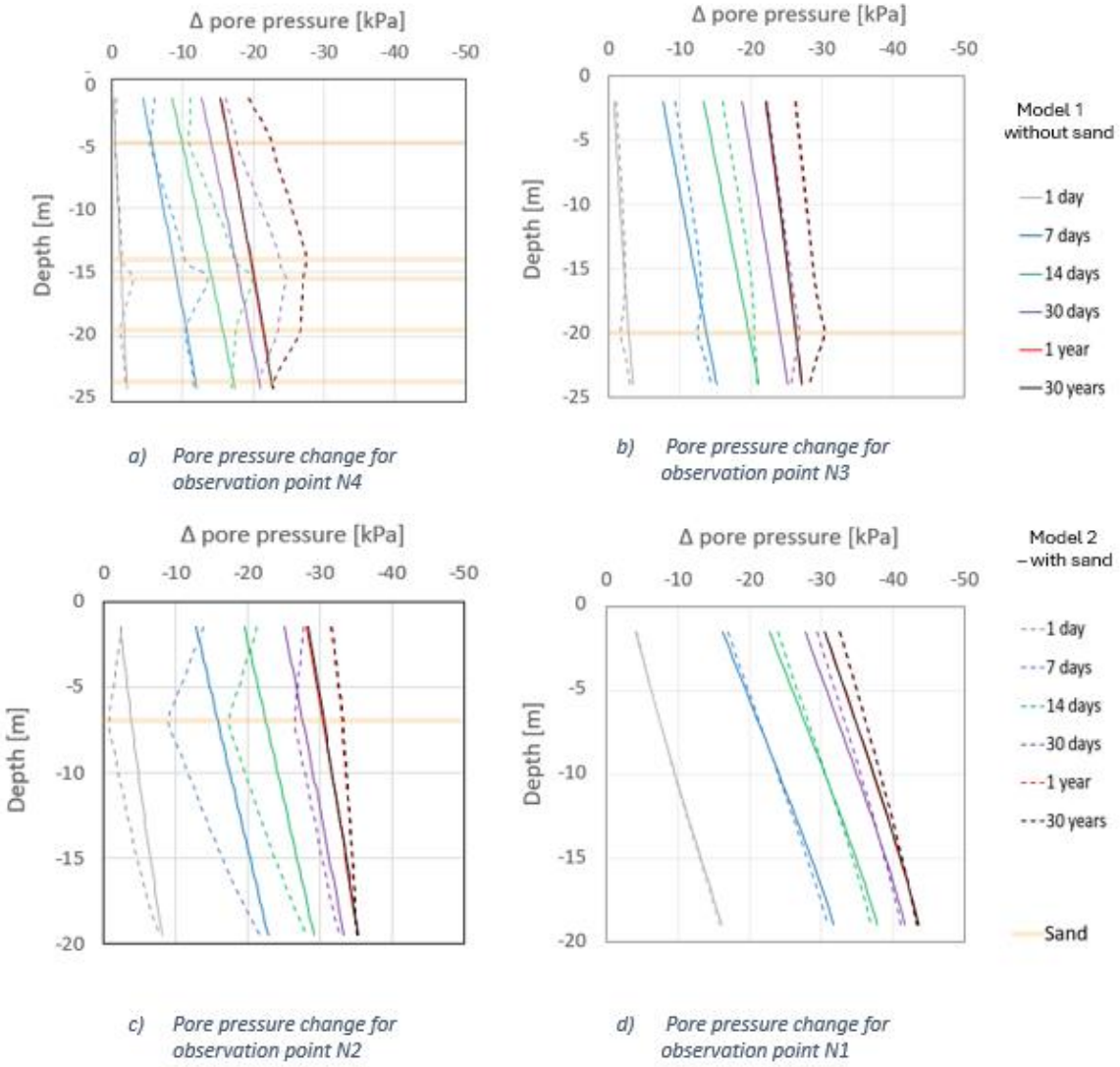

Figure 11. The change in pore pressure for each stress period, compared to the pore pressure before the leakage to the excavation, for the northern observation points N1-N4.

In the southern observation points differences in pore pressure reduction over time can be seen between the models (Figure 12). However, in contrast to the changes at the northern observation points the long-term pore pressure reduction at this side is not always higher for the model including sand. At observation point S4 and S3 (Figure 12a and b) the pore pressure reduction in the clay is lower for model 2 – with sand. This could be caused by a higher inflow at the southern border due to the constant head boundary. However, the lower reduction also indicates higher heads at these points which means a lower gradient and thus lower inflow. The difference of inflow between the models is also only about 3 l/min (see Appendix B) and it is likely that this difference in flow is mainly in the *Mölndalsån* river valley. It is therefore more likely that the difference is due to that sand layers are creating more recharge paths from the upper to the lower aquifer and thereby results in smaller changes in the pressure level.

At observation point S3 (Figure 12 c) the pressure reduction for *model 2 – with sand* is the same for both the lower aquifer and the sand lens, suggesting that they are connected, and the sand lens is acting as an extension of this aquifer. It can also be seen that the reduction in the model with sand is higher for the upper aquifer indicating that there could be sand layers acting as in Case II in Figure 5, where the sand is connecting the upper and lower aquifer thus creating recharge to the lower from the upper aquifer, in the surrounding area.

In contrast to the other observation point there is similar difference between the two models at the bottom of the graph for observation point S4 (Figure 12d). This is likely since there are no glacial till in this observation point. However, the sand lens seems to represent Case II in Figure 5, and therefore the pore pressure reduction in the clay is higher for the model including sand.

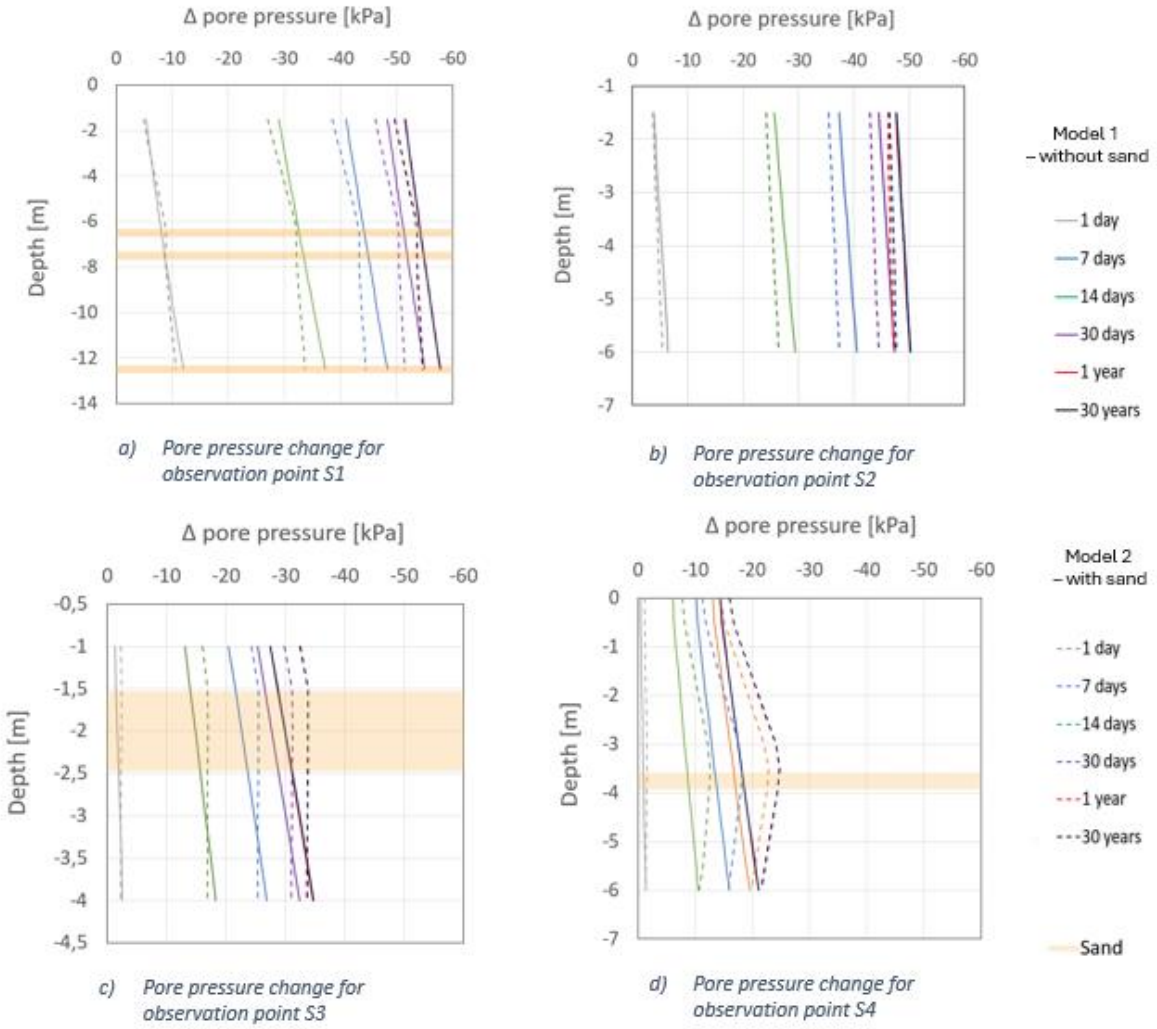

Figure 12. The change in pore pressure for each stress period, compared to the pore pressure before the leakage to the excavation, for the northern observation points S1-S4.

5 Discussion

The result from the two groundwater flow models shows that there are significant differences in pore pressure reduction and pressure levels when including local and permeable sand layers in the hydrological model. The differences in reduction patterns observed between the models with and without sand lenses highlight the complex behaviour of these geological formations. The influence of sand layers on pore pressure reduction was found to vary over time depending on their location and possible connection to other permeable layers. Sand layers connected to the lower aquifer were observed to function as an extension of this aquifer. Under stress, they serve as drainage channels within the clay sequence, resulting in increased reduction rates and greater changes in pore pressure within the surrounding clay. Isolated sand layers were found to reduce the short-term reduction rate of pore pressure in surrounding clay, but long-term they had little effect on the magnitude. Sand layers were also found to work as an extended recharge pathway if connected to both the upper and lower aquifers, reducing the drawdown in the lower aquifer and reducing the water levels in the upper aquifer.

There are uncertainties surrounding the differences in the results when including and excluding sand layers. *Model 2 – with sand* represents just one possible realization of the underlying model interbedded sand layers. As the result suggested that the impact of the sand layers varies based on their position and connectivity to the upper or lower aquifer, it would be beneficial to assess the outcomes with additional conceptualisations of the sand lenses, thus evaluating multiple equally probable realizations of the sand layer distribution. Case I's sand lenses can for example have a significantly higher impact on the pore pressure reduction if they are in direct contact with or close to the excavation, which is not the case in the geological model used in this thesis.

There are also uncertainties regarding the conceptualisation of hydrogeology in the area. The hydrological conceptualisation is highly simplified to focus on the main purpose of this report. However, these simplifications have also resulted in differences between the models. For example, boundary conditions with constant heads enable different inflow and outflow through the models, which complicates the evaluation of the differences caused by the sand lenses. However, this is considered necessary to reduce the complexity of the models. For example, a constant inflow and outflow for the models would have to be adapted for each stress period since the gradient in the case of a head reduction during the excavation would lead to a higher inflow. This can be seen in the result where the constant head at the southern border leads to an increase in inflow over time. Groundwater modelling in urban areas is complex since so many different factors affect the natural water balance. One of those challenges is assessing the inflow and outflow in the area taking into account drainage structures, such as tunnels and stormwater management systems that divert water. Additionally, recharge from leaking water pipes is a variable that must be considered, as it affects groundwater levels in the area. Hard surfaces, such as asphalt and concrete, also affect water movement and infiltration into the ground. Taking all these factors into account is necessary to develop an accurate groundwater model for urban areas but is in many cases difficult to estimate.

The excavation shaft has in this report been represented through the pre-coded packages horizontal flow barriers (HFB) and drains (DRN). This has been shown to be a reasonable way to represent the shaft. The retaining walls of the excavation have been represented by the HFB which enables evaluation of the actual area of the excavation which could be in direct contact with sand layers. This is an important aspect for examining the influence of sand layers since the results demonstrate that the reaction to pore pressure response varies depending on the position of the sand layers. However, in this report there were no sand layers in direct contact with the excavation and therefore no great

differences could be seen in the drawdown. It could therefore be of interest to further examine how the sand lenses are affecting the pore pressure reduction if connected to the walls of the excavation.

Another improvement that would be interesting to evaluate is a more realistic scenario for the shaft where a step wise approach is used. In this study the results show an effect from the excavation from day 1 even for observation point N4 and S4 furthest from the excavation. This is because the excavation is extending down to the lower aquifer where the high conductivity leads to instant response in the lower aquifer. However, to mimic a more realistic construction period the drains could be activated in different stress periods at different depths. This could help further investigation on how the sand lenses are affecting the pore pressure due to their location. A disadvantage with the way that the excavation was simulated is that it is a manual iterative process as the expected outflow cannot be specified. Instead, the flow governing parameters in DRN and HFB had to be adjusted to represent a reasonable leakage into the shaft.

The voxel model approach has been shown to be a possible method to include and well represent thin sand layers within the clay sequence. The voxel approach is beneficial for dealing with sand layers within the clay sequence due to its ability to capture local heterogeneity in the stratigraphy. As the results show that there are sand lenses acting as intermediate aquifers the voxel model has proven to capture these local heterogeneities in the clay. The main drawback with the voxel model is that the model becomes complex and generally large which leads to longer time consumption for the simulations. In this study the models resulted in over 8 million cells and simulations took between 20 and 120 minutes to run on a PC due to the complexity of the model, depending on the number of time steps used for each stress period. This could be seen as too time consuming when various parameters should be changed to fully understand the impact they have on the result. However, since groundwater modelling is often used to understand how external stresses can affect groundwater drawdown where the effects of subsidence can have enormous consequences and costs, the time invested should not be a concern.

The model results clearly show that the two models govern different pace and magnitude of groundwater impact induced by leakage to the open shaft. The differences in pore pressure for the two models indicate that by neglecting these sand lenses when predicting groundwater impacts and subsequent pore pressure change, the impact may be both over- and underestimated. Since pore pressure reduction in soft soils can trigger risks such as subsidence and subsequently damage to the built environment, the prediction of the magnitude of pore pressure reduction is of great importance when conducting risk analysis and thus risk assessment. When including sand lenses in the geological conceptualisation, a better risk analysis can be carried out, which in turn provides better conditions for managing the risks. A valid representation of the geological conditions of the area is thus crucial for effective risk management. This is both since the knowledge about the pace and magnitude of the pore pressure changes in the clay and the understanding of the water's flow paths is improved. If it is known that the pore pressure reduction in the clay is extensive in a part of the influence area, this must be considered, and measures to reduce the pace of consolidation should be implemented in the early stages of the excavation process. If the pore pressure reduction is slower instead, there is more room to reduce the impact later in the process. This means that the management of groundwater-related risks such as settlement damage is improved because the inclusion of sand lenses provides information about the course of time that is more accurate than with a simplified geological model. Inclusion of sand lenses can also provide an improved picture of local variations and thus enable evaluation of the placement of possible measures such as infiltration wells.

6 Conclusion

The main conclusions from this thesis are:

- The voxel approach has been shown to be a reasonable approach to well represent local heterogeneity within the stratigraphy.

- Inclusion of sand lenses in clay deposits in modelling of groundwater flow has been shown to provide significantly different results of pore water pressure compared to ignoring these sand lenses. This shows that it is important to take the sand layers into account in groundwater modelling. The presence of thin sand layers embedded within clay is common in areas with a history of varying sea levels, and inclusion of these geologic uncertainties has been shown to be important for improved understanding and prediction of groundwater flows.

- There are different impacts of the sand layers depending on their location and connectivity to the upper and/or lower aquifer. This leads to different effects as the pore pressure can both increase and decrease, hence presenting both positive and negative impact in terms of settlements.

- When excluding these types of geological uncertainties, there is a risk of underestimating possible subsidence. This can, for example, lead to costly damage and repairs to buildings and infrastructure.

References

Anderson, M. P., Woessner, W. W., & Hunt, R. J. (2015). *Applied groundwater modelling: simulation of flow and advective transport*. Academic press.

Baalousha, H. (2009). Fundamentals of groundwater modelling. *Groundwater: Modelling, Management and Contamination; Konig, LF, Weiss, JL, Eds*, 149-166.

Bakker, M., Post, V., Langevin, C. D., Hughes, J. D., White, J. T., Starn, J., & Fienen, M. N. (2016). Scripting MODFLOW model development using Python and FloPy. *Groundwater*, *54*(5), 733-739.

Bastante, F., Ordóñez, C., Taboada, J., & Matías, J. (2008). Comparison of indicator kriging, conditional indicator simulation and multiple-point statistics used to model slate deposits. *Engineering Geology*, *98*(1-2), 50-59.

Bjerrum, L. (1967). Engineering geology of Norwegian normally-consolidated marine clays as related to settlements of buildings. *Geotechnique*, *17*(2), 83-118.

Boone, S. J. (1996). Ground-movement-related building damage. *Journal of geotechnical engineering*, *122*(11), 886-896.

Boyce, S. E., Nishikawa, T., & Yeh, W. W. (2015). Reduced order modelling of the Newton formulation of MODFLOW to solve unconfined groundwater flow. *Advances in Water Resources*, *83*, 250-262.

Doherty, J. (2015). *Calibration and uncertainty analysis for complex environmental models*. Watermark Numerical Computing Brisbane, Australia.

Doherty, J. E., & Hunt, R. J. (2010). *Approaches to highly parameterized inversion: a guide to using PEST for groundwater-model calibration* (Vol. 2010). US Department of the Interior, US Geological Survey Reston, VA, USA.

Enemark, T., Andersen, L. T., Høyer, A.-S., Jensen, K. H., Kidmose, J., Sandersen, P. B., & Sonnenborg, T. O. (2022). The influence of layer and voxel geological modelling strategy on groundwater modelling results. *Hydrogeology Journal*, *30*(2), 617-635.

Goovaerts, P. (1999). Geostatistics in soil science: state-of-the-art and perspectives. *Geoderma*, *89*(1-2), 1-45.

Harbaugh, A. W. (2005). *MODFLOW-2005, the US Geological Survey modular ground-water model: the ground-water flow process* (Vol. 6). US Department of the Interior, US Geological Survey Reston, VA, USA.

Hill, M. C., & Tiedeman, C. R. (2006). *Effective groundwater model calibration: with analysis of data, sensitivities, predictions, and uncertainty*. John Wiley & Sons.

Huggenberger, P., & Epting, J. (2011). Settings in Urban Environments. *Urban Geology: Process-Oriented Concepts for Adaptive and Integrated Resource Management*, 5-13.

Jørgensen, F., Høyer, A.-S., Sandersen, P. B., He, X., & Foged, N. (2015). Combining 3D geological modelling techniques to address variations in geology, data type and density–An example from Southern Denmark. *Computers & geosciences*, *81*, 53-63.

Jørgensen, F., Møller, R. R., Sandersen, P. B., & Nebel, L. (2010). 3-D geological modelling of the Egebjerg area, Denmark, based on hydrogeophysical data. *GEUS Bulletin*, *20*, 27-30.

Larsson, R., & Sällfors, G. (1995). Sättningsegenskaper i lös lera på grund av geologisk avsättning och'åldring'. In: Statens geotekniska institut.

Lundqvist, J. (1983). The glacial history of Sweden. In J. Ehlers (Ed.), *Glacial deposits in north-west Europe* (pp. 77-82). Rotterdam, Netherlands: Balkema.

McDonald, M.G. & Harbaugh, A.W. (1983). *A modular three-dimensional finite-difference ground-water flow model*. Open-File Report 83-875. U.S. Geological Survey.

Moya, C. E., Raiber, M., & Cox, M. E. (2014). Three-dimensional geological modelling of the Galilee and central Eromanga basins, Australia: New insights into aquifer/aquitard geometry and potential influence of faults on inter-connectivity. *Journal of Hydrology: Regional Studies*, *2*, 119-139.

Niswonger, R. G., Panday, S., & Ibaraki, M. (2011). MODFLOW-NWT, a Newton formulation for MODFLOW-2005. *US Geological Survey Techniques and Methods*, *6*(A37), 44.

Persson, J. (2007). *Hydrogeological Methods in Geotechnical Engineering: Applied to settlements caused by underground construction*. Chalmers University of Technology.

Polomčić, D., Hajdin, B., Stevanović, Z., Bajić, D., & Hajdin, K. (2013). Groundwater management by riverbank filtration and an infiltration channel: the case of Obrenovac, Serbia. *Hydrogeology Journal*, *21*(7), 1519-1530.

Refsgaard, J. C., Christensen, S., Sonnenborg, T. O., Seifert, D., Højberg, A. L., & Troldborg, L. (2012). Review of strategies for handling geological uncertainty in groundwater flow and transport modelling. *Advances in Water Resources*, *36*, 36-50.

Refsgaard, J. C., Henriksen, H. J., Harrar, W. G., Scholten, H., & Kassahun, A. (2005). Quality assurance in model based water management–review of existing practice and outline of new approaches. *Environmental modelling & software*, *20*(10), 1201-1215.

Refsgaard, J. C., Van der Sluijs, J. P., Brown, J., & Van der Keur, P. (2006). A framework for dealing with uncertainty due to model structure error. *Advances in Water Resources*, *29*(11), 1586-1597.

Ross, J. L., Ozbek, M. M., & Pinder, G. F. (2009). Aleatoric and epistemic uncertainty in groundwater flow and transport simulation. *Water Resources Research*, *45*(12).

SGU (2021). *Göteborgsområdets berggrund, jordarter och geologiska utveckling.*

Stafleu, J., Maljers, D., Gunnink, J., Menkovic, A., & Busschers, F. (2011). 3D modelling of the shallow subsurface of Zeeland, the Netherlands. *Netherlands Journal of Geosciences*, *90*(4), 293-310.

Sundell, J. (2016). *Risk Estimation of Groundwater Drawdown in Subsidence Sensitive Areas* Chalmers Tekniska Hogskola (Sweden)].

Sundell, J. (2018). *Risk assessment of groundwater drawdown in subsidence sensitive areas*. Chalmers Tekniska Hogskola (Sweden).

Sundell, J., Haaf, E., Tornborg, J., & Rosén, L. (2019). Comprehensive risk assessment of groundwater drawdown induced subsidence. *Stochastic Environmental Research and Risk Assessment*, *33*(2), 427-449.

Sällfors, G. (2013). *Geoteknik* (Vol. 5). Cremona Förlag vid Chalmers tekniska högskola.

Tartakovsky, D. M. (2013). Assessment and management of risk in subsurface hydrology: A review and perspective. *Advances in Water Resources*, *51*, 247-260.

Trafikverket (2016). *PM Beskrivning Hydromodell - Underlagsdokument till PM Hydrogeologi, ansökan om tillstånd enligt miljöbalken för anläggandet av Västlänken och Olskroken planskildhet.*

Walker, W. E., Harremoës, P., Rotmans, J., Van Der Sluijs, J. P., Van Asselt, M. B., Janssen, P., & Krayer von Krauss, M. P. (2003). Defining uncertainty: a conceptual basis for uncertainty management in model-based decision support. *Integrated assessment*, *4*(1), 5-17.

Xiao, T., Zhang, L.-M., Li, X.-Y., & Li, D.-Q. (2017). Probabilistic stratification modelling in geotechnical site characterization. *ASCE-ASME Journal of Risk and Uncertainty in Engineering Systems, Part A: Civil Engineering*, *3*(4), 04017019.

Zetterlund, M., Norberg, T., Ericsson, L. O., & Rosén, L. (2011). Framework for value of information analysis in rock mass characterization for grouting purposes. *Journal of Construction Engineering and Management*, *137*(7), 486-497.

Appendix A

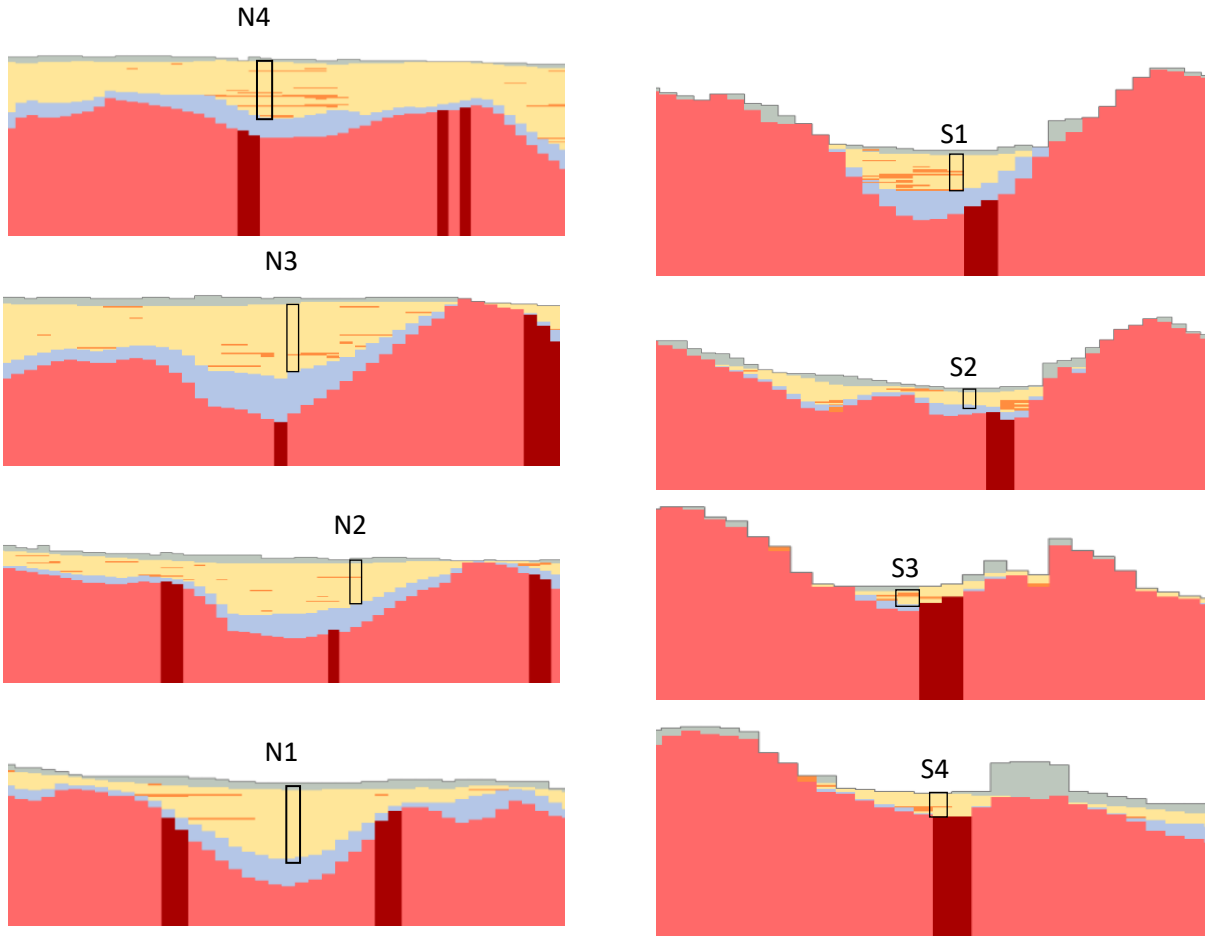

Figure 13. Illustration of the area of which the pore pressure reduction has been evaluated.

Appendix B

MODEL 1 - without sand

In (m3/ day)	0 days	1 day	7 days	14 days	30 days	1 year	30 years
storage	34,4	303,3	125,5	67,8	23,3	0,6	0
constant head	250,4	250,0	255,3	259,6	270,2	282,1	282,4
drains	0	0	0	0	0	0	0
river leakage	18,1	18,5	19,5	20,3	21,0	21,4	21,5
recharge	181,4	181,4	181,4	181,4	181,4	181,4	181,4
total in	484,3	753,2	581,7	529,1	495,9	485,5	485,3
Out (m^3/day)							
storage	34,9	4,1	0	0	0	0	0
constant head	397,6	394	352,4	318,2	297,1	292,3	292,2
drains	0	305,3	183,7	168,3	158,6	154,3	154,2
river leakage	51,8	49,8	45,6	42,6	40,2	38,9	38,9
recharge	0	0	0	0	0	0	0
total out	484,3	753,2	581,7	529,1	495,9	485,5	485,3

MODEL 2 - with sand

In (m3/ day)							
storage	33,3	319	137,6	76,8	27,8	0,7	0
constant head	254,4	254,2	259,4	264	273,9	287,3	287,8
drains	0	0	0	0	0	0	0
river leakage	18,1	18,7	19,8	20,6	21,4	21,9	21,8
recharge	181,4	181,4	181,4	181,4	181,5	181,4	181,4
total in	487,2	773,3	598,2	542,8	504,6	491,3	491
Out (m^3/day)							
storage	24,9	0,9	0	0	0	0	0
constant head	410,1	407,3	364,3	328,3	302,7	295,9	295,7
drains	0	315,4	188,7	172,4	162,4	157,5	157,4
river leakage	52,2	49,7	45,2	42,1	39,5	37,9	37,9
recharge	0	0	0	0	0	0	0
total out	487,2	773,3	598,2	542,8	504,6	491,3	491

Appendix C

Script for the translation of the geological model

```
import numpy as np
import pandas as pd
import matplotlib.pyplot as plt

## Open elevation file:
top = np.loadtxt("C:/Users…… -MedIndicatorSand.dat", delimiter = ",")

top = pd.DataFrame(top, columns = ['x','y','z','i'])

## Exclude i=6, - above ground surface
top2 = top[top['i'] != 6] #!= not equal to

## Print the data
top2.head()
```

```
          x          y          z    i
0  148390.0  6396740.0 -65.892269  7.0
1  148400.0  6396740.0 -65.892269  2.0
2  148410.0  6396740.0 -65.892269  2.0
3  148420.0  6396740.0 -65.892269  2.0
4  148430.0  6396740.0 -65.892269  7.0
```

```
## Remake the "cordinats" into rows and columns

x = top2['x'].values
y = top2['y'].values
z = top2['z'].values
i = top2['i'].values

X = (x-x.min())/10
Y = -(y-y.max())/10
Z = z
I = i

## Create the new dataFrame with rows and columns

new_top = pd.DataFrame({
    'X': X,
    'Y': Y,
    'Z': z,
    'i': i
})

## Print the new data frame
new_top.head()
```

```
     X      Y          Z    i
0  0.0  157.0 -65.892269  7.0
1  1.0  157.0 -65.892269  2.0
2  2.0  157.0 -65.892269  2.0
3  3.0  157.0 -65.892269  2.0
4  4.0  157.0 -65.892269  7.0
```

Create the topografy

```
## Group the rows by 'x' and 'y' and extract the maximum 'z' value for each group
max_elevations = new_top.groupby(['X', 'Y'])['Z'].max().reset_index()

## Print the resulting DataFrame
print(max_elevations) # 158*173 = 27334, check that the number of rows is correct
```

```
           X      Y          Z
0        0.0   -0.0   1.107731
1        0.0    1.0   1.607731
2        0.0    2.0   1.607731
3        0.0    3.0   2.107731
4        0.0    4.0   2.607731
...      ...    ...        ...
27329  172.0  153.0  20.607731
27330  172.0  154.0  20.607731
27331  172.0  155.0  20.107731
27332  172.0  156.0  20.107731
27333  172.0  157.0  19.607731

[27334 rows x 3 columns]
```

```
## Determine the number of rows and columns

nrow = int(max_elevations['Y'].max()) + 1
ncol = int(max_elevations['X'].max()) + 1

## Creat and initialize the NumPy array with a default value (e.g., -35.0)
mtop = np.full((nrow, ncol), -35.0, dtype=float)

## Iterate through the DataFrame to update the array with non-default values
for index, row in max_elevations.iterrows():
    x = int(row['X'])
    y = int(row['Y'])
    z = row['Z']
    mtop[y, x] = z

print("Maximum and minimum elevation of mtop:",(mtop.max(), mtop.min())) ## Check
that the default value is not the lowest
print("mtop shape:", mtop.shape) # mtop should be 2D with the shape as (rows, col)
```

```
Maximum and minimum elevation of mtop: (81.1077313694, -0.3922686306)
mtop shape: (158, 173)
```

```
plt.imshow(mtop)
```

```
<matplotlib.image.AxesImage at 0x1827942e890>
```

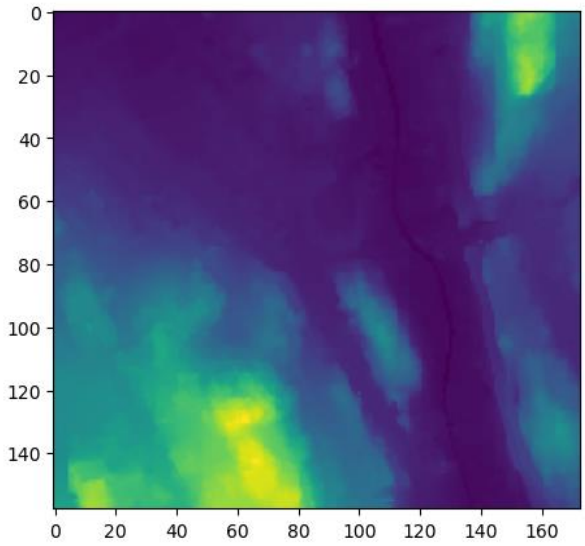

Creat the cell type array

```
## Create a new dataFrame with number of layers
## and 'rank' Z that contains the corresponding layer for each row and column (0 f
or the highest 'z', and so on..)

## Group the DataFrame by 'x' and 'y' and rank the 'z' values within each group
new_top['rank'] = new_top.groupby(['X', 'Y'])['Z'].rank(ascending=False, method='f
irst') - 1


new_top.head()
```

```
     X      Y          Z    i   rank
0  0.0  157.0 -65.892269  7.0  225.0
1  1.0  157.0 -65.892269  2.0  224.0
2  2.0  157.0 -65.892269  2.0  224.0
3  3.0  157.0 -65.892269  2.0  223.0
4  4.0  157.0 -65.892269  7.0  224.0
```

```
## Determine the dimensions of the grid, (layer, row, column)
nlay = int(new_top['rank'].max()) + 1  # Add 1 to account for zero-based indexing
nrow = int(new_top['Y'].max()) + 1
ncol = int(new_top['X'].max()) + 1

## Creating the numpy array and initialize with a default value (e.g., 10)
cell_typ = np.full((nlay, nrow, ncol), 8)

## Iterate through the DataFrame to update the array with non-default values
for index, row in new_top.iterrows():
    x = int(row['X'])
    y = int(row['Y'])
    z = int(row['rank'])
    d = row['i']
    cell_typ[z, y, x] = d

## replace all the default values with the indicator for bedrock (i=2)
## This since the array creates 295 layers from the ground surface -> layers with
no i but all of them are bedrock.
cell_typ[cell_typ == 8] = 2
```

```
## Plot cell_typ for layer 1
fig = plt.figure(figsize=(5, 5))
plt.imshow(cell_typ[0, :, :])
```

```
<matplotlib.image.AxesImage at 0x18214057490>
```

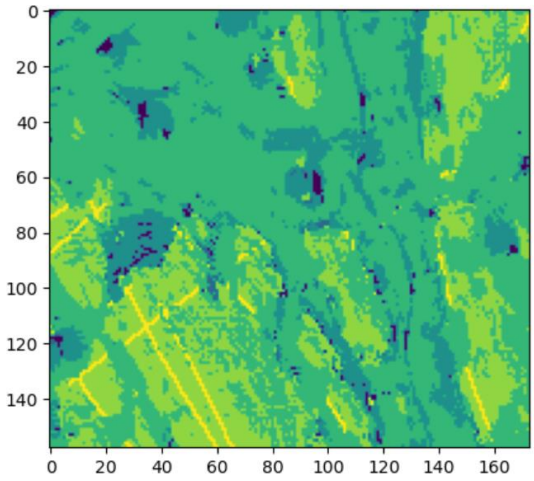

Appendix D

```
import os
import flopy
import numpy as np
import pandas as pd
import matplotlib.pyplot as plt
import flopy.utils.binaryfile as bf
import flopy.plot as fp
```

Step 1

```
## Define the cells

cellH = 10
nCols = 173
nRows = 158

## Insert topography

mtop = np.load('C:/Users……. mtop.npy')

mtop = mtop # - 0.392268631

print("Maximum and minimum elevation of mtop:",(mtop.max(), mtop.min()))
print("mtop shape:", mtop.shape) # mtop should be 2D with the shape as (rows, col)

Maximum and minimum elevation of mtop: (81.1077313694, -0.3922686306)
mtop shape: (158, 173)

#plt.imshow(mtop)

## Assign the name of the model
modelname='STORmedSandNY'

## Floder where the results are stored
model_ws= 'C:/Users……STORmedSandNY'

## Where the executable files are stored
exe_name='C:/Users…….MODFLOW-NWT/bin/MODFLOW-NWT_64.exe'

## Create the model
mf = flopy.modflow.Modflow(modelname, exe_name=exe_name, version="mfnwt",model_ws=
model_ws)

## Input data
zbot = -65.892269
layer_thickness = 0.5
mtop2 = mtop + 0.25

nLays =int(np.ceil((mtop.max()-zbot)/layer_thickness))

#print(nLays)

c=nLays*layer_thickness
d=int(np.ceil(mtop.min()-c))

#print(d)
```

```
## define the bottom
botm = np.empty((nLays+1, nRows, nCols)) # nLays +1
for k in range(nLays+1): # nLays +1
    botm[k,:,:] = (mtop2-layer_thickness) - k*layer_thickness
    botm[-1,:,:] = d-2.392268631

#print(mtop2)
#print(botm[-1])
#print("botm shape", botm.shape)
```

DIS

```
# Transient
nper = 7
perlen = [1, 1, 6, 7, 16, 335, 10585]
#nstp = [1, 1, 1, 1, 1, 1, 1]
nstp = [1, 1, 6, 7, 16, 11, 30]
steady = [False, False, False, False, False, False, False]

#Transient
dis = flopy.modflow.ModflowDis(mf, nlay=nLays, nrow=nRows, ncol=nCols, delr=cellH,
delc=cellH, top=mtop2, botm=botm[1:], laycbd=0, itmuni=4, lenuni=2, nper=nper, ste
ady=steady, perlen=perlen, nstp=nstp)
```

UPW - cell type

```
cell_typ = np.load('C:/Users/Axeen/Onedrive - Chalmers/Desktop/GWmod/MT-viktiga/np
y/cell_typSTORm7.npy')

hk = np.zeros([nLays,nRows,nCols])
ss = np.zeros([nLays,nRows,nCols])
sy = np.zeros([nLays,nRows,nCols])
vk = np.zeros([nLays,nRows,nCols])

## 1 Sand / Clay
hk[cell_typ == 1] = 3.048   # [m/d] Clay: 0.00009 m/d -> 1,0E-9 m/s, Sand: same as
moraine
vk[cell_typ == 1] = 3.048   # [m/d]
ss[cell_typ == 1] = 1.5e-4  # [1/m]
sy[cell_typ == 1] = 0.1     # [1/m]

# 2 Bedrock
hk[cell_typ == 2] = 0.0035   # [m/d] 0.0035 - 0.01728 m/d -> 0,4-2,0E-7 m/s
vk[cell_typ == 2] = 0.0035   # hk=vk
ss[cell_typ == 2] = 4e-7
sy[cell_typ == 2] = 0.001

## 3 Till/Lower aquifer
hk[cell_typ == 3] = 3.048    # 1.73-6.05 m/d -> 2-7E-5 m/s  (0.864-8.64 m/d
vk[cell_typ == 3] = 3.048    # vk=hk
ss[cell_typ == 3] = 1.5e-4   #
sy[cell_typ == 3] = 0.1

## 4 Clay
hk[cell_typ == 4] = 0.000086  # [m/d] Clay: 0.00009 m/d -> 1,0E-9 m/s
vk[cell_typ == 4] = 0.000043  # [m/d] 0.00004 m/d ->
ss[cell_typ == 4] = 1e-7
sy[cell_typ == 4] = 0.001

## 5 Fill
```

```
hk[cell_typ == 5] = 0.864    # [m/d] -> 1,0E-5 m/s
vk[cell_typ == 5] = 0.432    # vk=hk/2
ss[cell_typ == 5] = 0.0001
sy[cell_typ == 5] = 0.07

## 6 Bedrock
hk[cell_typ == 6] = 0.0035    # [m/d] 0.0035 - 0.01728 m/d -> 0,4-2,0E-7 ms
vk[cell_typ == 6] = 0.0035    # vk=hk
ss[cell_typ == 6] = 4e-7
sy[cell_typ == 6] = 0.001

## 7 Fracture zones
hk[cell_typ == 7] = 0.432    # 0,02-0.43 m/d -> 0.2-5 E-6
vk[cell_typ == 7] = 0.432    # vk=hk
ss[cell_typ == 7] = 4e-7
sy[cell_typ == 7] = 0.001

hk[(cell_typ == 4) & (nLays < 2)] = 0.864
vk[(cell_typ == 4) & (nLays < 2)] = 0.432
hk[(cell_typ == 1) & (nLays < 2)] = 0.864
vk[(cell_typ == 1) & (nLays < 2)] = 0.432

upw = flopy.modflow.ModflowUpw(mf, hk=hk, vka=vk, ss=ss, sy=sy)

## Illustration of crossection, check hk, vk, cell_typ

fig = plt.figure(figsize=(20, 5))
ax = fig.add_subplot(1, 1, 1)
modelxsect = flopy.plot.PlotCrossSection(model=mf, line={'row':90})
linecollection = modelxsect.plot_grid()
modelxsect.plot_array(hk)
```

```
<matplotlib.collections.PatchCollection at 0x16452242a50>
```

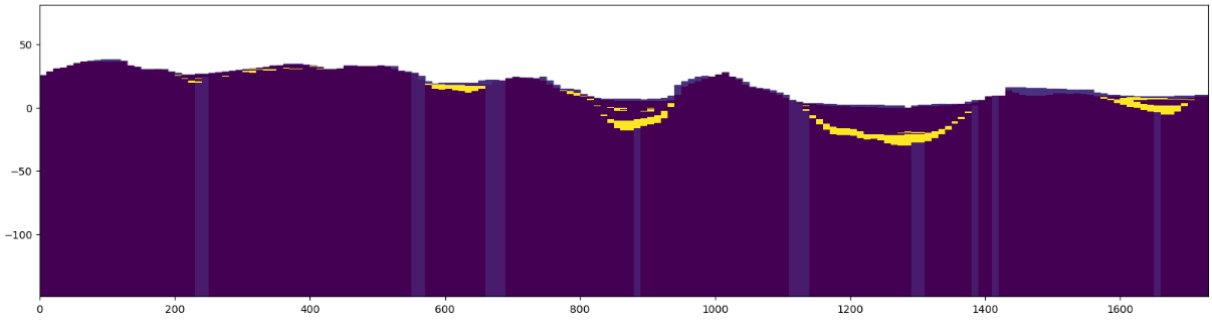

Step 2

BAS - ibound and strt

```
## Boundaries and strating conditions - BAS

## Load starting heads and no flow boundaries
strt_head = np.load('C:/Users……strtmed.npy')
boundary = np.load('C:/Users……boundary.npy')

## Create boundary condition at level -70 to no flow
botten1 = np.where((botm[0:295,:,:] > -70),1,0)
```

```
## Combine noflow at mountain and bottom
general_B = np.where((botten1[0:295,:,:] == 0) | (boundary[0:295,:,:] == 0), 0, 1)

## Constant head boundary at southern and northen border
NB1 = np.where((botm[0:295,0,0:137] > -70),-1,0)
SB3 = np.where((botm[0:295,-1,83:170] > -70),-1,0)

## ibounds - boundary conditions
ibound = np.ones((nLays, nRows, nCols), dtype=np.int32)
ibound[:,:,:] = general_B
ibound[:,0,0:137] = NB1
ibound[:,-1,83:170] = SB3

## staring head values
strt = np.ones((nLays, nRows, nCols), dtype=np.float32)
strt[:,:,:] = strt_head
strt[:,0,0:137] = 0

bas = flopy.modflow.ModflowBas(mf, ibound=ibound, strt=strt)

## Plot ibound for layer 1
fig = plt.figure(figsize=(5,5))
ax = fig.add_subplot(1,1,1, aspect = 'equal')
modelmap = flopy.plot.PlotMapView(model =mf, layer = 0, ax=ax)
qm = modelmap.plot_ibound()

## Plot strt for layer 1
fig = plt.figure(figsize=(5, 5))
plt.imshow(strt[0, :, :], vmin=-5)
```

```
<matplotlib.image.AxesImage at 0x1d4bd6b6750>
```

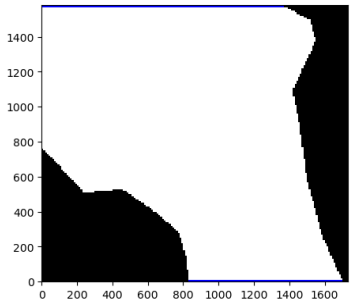

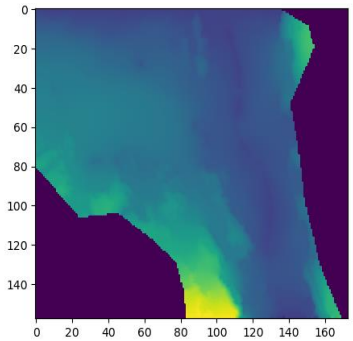

RIV - Mölndalsån

```
river = pd.read_csv("C:/Users……River.csv",sep=";", index_col=0)

row = river['y'].values
```

```
col = river['x'].values
lay = river['nLay'].values
head_river= mtop[row,col]
con =river['c'].values
Rbot=head_river-0.5

spd_RIV= {
    0: np.column_stack([lay, row, col, head_river, con, Rbot]),
}

riv = flopy.modflow.ModflowRiv(mf, stress_period_data=spd_RIV)
```

RCH - recharge

```
## Recharge - RCH
## XXX mm/year -> XXX/(1000*365) m/day

rech = np.ones((1, nRows, nCols), dtype=np.float32)

for lay in range(1):
    for row in range(nRows):
        for col in range(nCols):
            if cell_typ[lay, row, col] == 4:
                rech[lay, row, col] = (0) #30/(1000*365)
            elif cell_typ[lay, row, col] == 1:
                rech[lay, row, col] = (0) #30/(1000*365)
            elif cell_typ[lay, row, col] == 6:
                rech[lay, row, col] = 90/(1000*365)
            else:
                rech[lay, row, col] = 30/(1000*365)

rech[:,82:88,78:92]=(0)

rech_data = {0: rech}
rch = flopy.modflow.ModflowRch(mf,rech=rech_data)

rch.plot()

[<Axes: title={'center': 'RECH stress period 1'}>]
```

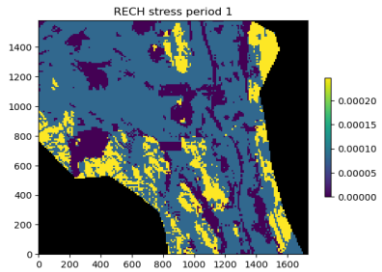

DRN - drains/excavation

```
## Drainage - DRN
## Creat the excavation (DRAINS) from excel dokument

List = pd.read_csv("C:/Users/Axeen/Onedrive - Chalmers/Desktop/GWmod/MT-viktiga/Ex
cel/excavationSTOR.csv",
                   sep=";", index_col=0)
#List.head()
```

```
layer = List['nLays'].values
row = List['nRows'].values
col = List['nCols'].values
elevation = List['z'].values - 0.3922686306
con = List['c'].values

## create stress period data for each stress period
spd_DRN = {
    1: np.column_stack([layer, row, col, elevation, con]),  # 1-> applies in the s
econd stress period
}

drn = flopy.modflow.ModflowDrn(mf, stress_period_data=spd_DRN)
```

HFB - Horizontal Flow Barriers

```
## Horizontal flow barrier - HFB
## Adding the Walls to the excavation
## Have no transient application, so the walls will be active in all stress period
s

List_HFB = pd.read_csv("C:/Users/Axeen/Onedrive - Chalmers/Desktop/GWmod/MT-viktig
a/Excel/WallsSTOR_berg.csv",
                       sep=";", index_col=0)
#List_HFB.head()

lay = List_HFB['lay'].values
row1 = List_HFB['row1'].values
col1 = List_HFB['col1'].values
row2 = List_HFB['row2'].values
col2 = List_HFB['col2'].values
hydchr = List_HFB['hydchr'].values

hfb_data = np.column_stack([lay, row1, col1, row2, col2, hydchr])

#print(hfb_data)

hfb = flopy.modflow.ModflowHfb(mf, hfb_data=hfb_data)
```

OC - Output controll

```
## Output controll - OC

## Transient
spd = {}
for kper in range(nper):
    for kstp in range(nstp[kper]):
        spd[(kper, kstp)] = [
            "SAVE HEAD",
            "SAVE BUDGET",
            "PRINT BUDGET",
        ]

oc =  flopy.modflow.ModflowOc(mf, stress_period_data = spd, compact = True)
```

NWT - Solver

```
# Solver - NWT (Newton)
nwt = flopy.modflow.ModflowNwt(mf ,maxiterout=250,linmeth=2,headtol=0.01,Continue=
False)
```

```
mf.write_input()

success, buff = mf.run_model()
if not success:
    raise Exception("MODFLOW did not terminate normally.")
```